

**ECONOMIC GEOLOGY
RESEARCH UNIT**

University of the Witwatersrand
Johannesburg

MOLECULAR AND ELEMENTAL ANALYSES OF THE
CARBONACEOUS MATTER IN THE GOLD- AND
URANIUM-BEARING VAAL REEF CARBON SEAMS,
WITWATERSRAND SEQUENCE

J.E. ZUMBERGE, A.C. SIGLEO, and B. NAGY

• INFORMATION CIRCULAR No. 128

UNIVERSITY OF THE WITWATERSRAND

JOHANNESBURG

MOLECULAR AND ELEMENTAL ANALYSES OF THE
CARBONACEOUS MATTER IN THE
GOLD- AND URANIUM-BEARING VAAL REEF CARBON SEAMS,
WITWATERSRAND SEQUENCE

by

J.E. ZUMBERGE, A.C. SIGLEO, and B. NAGY

*(Laboratory of Organic Geochemistry,
University of Arizona, Tucson, U.S.A.)*

ECONOMIC GEOLOGY RESEARCH UNIT

INFORMATION CIRCULAR No. 128

December, 1978

INFORMATION CIRCULAR No. 128

The information contained herein has been reprinted from *Minerals Science and Engineering*, Volume 10, No. 4, October, 1978, with the kind permission of the Editor, Dr. E.H. Wainwright, of the National Institute for Metallurgy, Randburg.

MOLECULAR AND ELEMENTAL ANALYSES OF THE
CARBONACEOUS MATTER IN THE
GOLD- AND URANIUM-BEARING VAAL REEF CARBON SEAMS,
WITWATERSRAND SEQUENCE

CONTENTS

	<u>Page</u>
Synopsis	223
Introduction	223
Analytical Methods and Results	224
<i>High-Vacuum Pyrolysis - Gas Chromatography -</i>	224
<i>Mass Spectrometry</i>	
<i>Electron Paramagnetic Resonance Spectroscopy</i>	230
<i>Carbon-Hydrogen Atomic Ratios</i>	232
<i>Scanning-Electron Microscopy and Electron</i>	233
<i>Microprobe Analyses</i>	
<i>Instrumental Neutron Activation Analyses</i>	237
Discussion	237
<i>Chemical Matrix of the Vaal Reef Kerogen</i>	237
<i>Search for Correlations Between Organic Constituents</i>	239
<i>and Uranium and Gold Contents</i>	
<i>Rare-Earth and Variable-Valance Elements</i>	239
<i>Chemical History of the Vaal Reef Kerogen</i>	242
Conclusions	244
Acknowledgements	245
References	245

* * * * *

JOHN E. ZUMBERGE, ANNE C. SIGLEO* AND BARTHOLOMEW NAGY

*Laboratory of Organic Geochemistry, Department of Geosciences, The University of Arizona,
Tucson, Arizona 85721, U.S.A.*

**Present Address: Department of Chemistry, University of Maryland, College Park, Maryland 20742, U.S.A.*

MOLECULAR AND ELEMENTAL ANALYSES OF THE CARBONACEOUS MATTER IN THE GOLD AND URANIUM BEARING VAAL REEF CARBON SEAMS, WITWATERSRAND SEQUENCE

SYNOPSIS

The thin Vaal Reef carbon seams consist of a complex, solid, and solvent insoluble, polymer-like substance, containing mainly hydrocarbons and some organic sulphur and oxygen compounds. These carbon seams are not pure carbon, e.g. graphite, and do not contain only hydrocarbons. According to modern terminology the Vaal Reef carbonaceous matter is most appropriately referred to as kerogen rather than carbon or thucholite. This kerogen is not the result of the polymerization of gaseous or liquid hydrocarbons, but rather of the polymerization of biochemicals from decayed, primitive Precambrian micro-organisms. These microbiota formed mats in which uranium minerals and gold became incorporated before burial under younger sediments. Organic geochemistry was first developed as a means to elucidate the nature and composition of petroleum and coal. Later it was successfully used in lunar sample, planetary surface, and meteorite studies as well as in investigations of kerogens in terrestrial sediments of various ages. Considering economic geology, organic geochemistry holds promise for elucidating the origin and helping in the exploration of carbonaceous ore deposits. The purpose of this report is to review some of the major current organic geochemical methods and to illustrate these by the analyses of the Vaal Reef kerogen. The samples were analysed by a directly connected high vacuum pyrolysis system-gas chromatograph-organic mass spectrometer. Additional analyses were performed by a combined scanning electron microscope-electron microprobe, by the techniques of electron paramagnetic resonance spectroscopy, and by neutron activation analysis. The majority of the pyrolysis breakdown products of the Vaal Reef kerogen are alkyl substituted aromatic hydrocarbons, low molecular weight aliphatic hydrocarbons, with some aromatic sulphur and aliphatic oxygen compounds. The dimethylnaphthalene pyrolysis products decreased in abundance relative to other alkynaphthalenes as uranium content increased. The evolution of the Vaal Reef kerogen from the original biochemicals of primitive micro-organisms apparently progressed through free radical reactions. The carbon seams contain from ten to one hundred times more organic free radicals than coal as was shown by electron paramagnetic resonance spectroscopy. Many of the organic free radicals are thought to have formed by irradiation emitted by uraninite. Examination of Vaal Reef carbon seams by scanning electron microscopy and concurrent electron microprobe analysis (including carbon analyses) revealed a complex organic-gold-clay system including different chemical paleo-microenvironments. Carbon-hydrogen atomic ratios of the Vaal Reef kerogen are generally similar to those of bituminous coals and increase as the clay content increases. Rare earth elements are present in the kerogen, probably in zircon and clay minerals as was shown by neutron activation analysis.

Dr John E. Zumberge received his B.S. degree in chemistry from The University of Michigan and obtained his M.S. and Ph.D. degrees in geochemistry from The University of Arizona. He is presently a Research Associate in the Department of Geosciences, the Laboratory of Organic Geochemistry, The University of Arizona. He has been investigating the geochemistry of kerogen and other organic substances in Precambrian rocks since 1971 and has published numerous articles on this subject.

Dr Anne C. Sigleo obtained her B.A. degree in anthropology and her M.S. degree in geology from the University of New Mexico and received her Ph.D. degree in geochemistry from The University of Arizona. Presently, she is a Research Associate in the Department of Chemistry, The University of Maryland. She has done extensive work with neutron activation analyses of geological samples and is currently analysing organic matter from Chesapeake Bay water.

Professor Bartholomew Nagy majored in chemistry for his undergraduate degree, obtained his M.A. degree in economic geology from Columbia University and his Ph.D. in geochemistry and mineralogy from The Pennsylvania State University. He initiated and headed the geophysical and geochemical petroleum Exploration Research Division of the Cities Service Research and Development Co. in Tulsa, Oklahoma prior to joining the faculty of the Department of Chemistry at Fordham University. Between 1962-68 he worked in the Department of Chemistry, University of California at San Diego and since 1968 at

the Department of Geosciences of The University of Arizona, where he is Chief Scientist of the Laboratory of Organic Geochemistry. He organized the Organic Geochemistry Division of the Geochemical Society, served as its first Chairman and subsequently as Councillor of the Geochemical Society. He was Chairman of the Section of Geological Sciences and served on the Council of The New York Academy of Sciences. He was selected by NASA as one of the Principal Investigators for the Apollo Lunar Sample Analysis Program and served on the Advisory Board of the Lunar Science Institute. He has published some 150 scientific articles and two books.

INTRODUCTION

Organic geochemistry deals with the nature and role of organic chemicals in the earth's lithosphere, hydrosphere, and atmosphere as well as in extraterrestrial environments, e.g., on the lunar surface and in certain meteorites, etc. For almost a century and a half, the term 'organic' no longer bears its initial connotation of 'biogenic' to chemists but now merely refers to carbon chemistry. Thus, certain

aspects of non-biological carbon chemistry, whether terrestrial or extraterrestrial, fall within the scope of organic geochemistry. However, most, if not all, organic matter in sedimentary rocks on earth is generally believed to have been derived from the ancient debris of plants and/or animals, with the possible exception of the disordered graphite in the ~ 3 800-million-year-old metasedimentary rocks from the Isua area, southwestern Greenland¹. The solid organic matter in sedimentary rocks generally occurs as kerogen. The term thucholite has been proposed originally to designate organic matter containing Th, U, O, and, of course, C and H. Unfortunately, in recent years this term has been used rather indiscriminately and to many earth scientists it no longer bears its original connotation. Kerogen, an organic solid that is insoluble in common organic solvents, is of interest to geochemists because most sedimentary rocks contain at least a few tenths of a per cent of this substance, finely disseminated throughout the mineral matrix, or occasionally in thin layers and laminae, such as in stromatolites. If one considers the total volume of sedimentary rocks in the Earth's crust, it becomes evident that kerogen is the most abundant terrestrial organic matter; its abundance is² approximately 2.5×10^{21} g. In organic geochemical studies it is preferable to analyse kerogen in sedimentary rocks rather than the solvent soluble organic substances because the latter may well have been introduced into permeable rocks any time after deposition. However, it is rather difficult and time-consuming to analyse kerogen because it is an insoluble, complex, and random-polymeric solid^{3,4}. Detailed procedures for kerogen analysis did not generally become available until relatively recently, spurred on by the U.S.A. space programme.

There is one question that can be raised at present. What is the significance of knowing the properties of kerogen to the understanding of geological events during the history of the earth? One answer is that kerogen chemistry is used increasingly in attempts to understand the evolution and nature of life during Precambrian time. More specifically elucidating prebiological (chemical) and subsequent biological evolution during the Early Precambrian is of increasing concern to fundamental research. The majority of the kerogenous sedimentary rocks that are studied in this context have been collected in southern Africa. Chemical evidence for life and life-supporting environments during the Early Precambrian can provide necessary support to micropaleontological observations of Archean microstructures because the earliest, primitive unicellular and non-nucleated organisms usually do not have distinctive morphological features or are poorly preserved⁵. Of course, the molecular structure of the vast majority of the original biochemicals incorporated within ancient sediments has been altered through microbial and subsequent diagenetic processes leading to the formation of kerogen. A few key organic compounds isolated from Precambrian kerogens must reflect known biochemical molecules if they are to be construed as 'biochemical fossils'^{4,6}. This is not always possible since many of the functional groups and even molecular carbon skeletons are obscured during the random polymerization of the original biochemical matter. Consequently, studies of the diagenetic and metamorphic histories of the sedimentary rocks containing organic compounds are important ancillary aspects to any type of organic geochemical research⁶.

What is more significant in the present context is that kerogen studies are important to at least two areas of economic geology. First, using extensive kerogen-rich sedimentary rocks for sources of fossil fuels is becoming economically feasible. Some of the sedimentary rocks rich in kerogen are the oil shales. Second, a number of ore minerals may be intimately associated with and concentrated in kerogen. In both cases, proper understanding of the properties of kerogen facilitates recovery and/or exploration. With the above reasoning in mind, the kerogen from the Precambrian Vaal Reef placer sediments (2.5×10^9 years old)⁷ of the Witwatersrand Sequence, South Africa, was studied, with the dual consideration of its significance to both economic geology and paleobiology.

ANALYTICAL METHODS AND RESULTS

The following methods were used to analyse the insoluble, solid Vaal Reef organic matter and its associated inorganic components:

(1) combined high vacuum pyrolysis-gas chromatography-mass spectrometry, (2) electron paramagnetic resonance spectroscopy, (3) elemental analyses for organic carbon and hydrogen, (4) combined scanning electron microscopy-electron microprobe analyses, and (5) instrumental neutron activation analyses.

High vacuum pyrolysis-gas chromatography-mass spectrometry

Pyrolysis is a technique often used by polymer chemists to break down a polymer into its components with the aid of thermal energy in an inert atmosphere (e.g. He) or *in vacuo*. This method must be used with prudence. When a polymer sample is heated in an inert atmosphere near atmospheric pressures, the 'hot' organic breakdown products have a statistically greater opportunity to collide with each other and recombine to form molecules that were never present in the polymer⁸. Pyrolysis of a small sample in vacuum ($\sim 10^{-6}$ torr) minimizes such secondary product syntheses. Following pyrolysis, the polymer degradation products must be identified; the most suitable technique of doing this at present is organic mass spectrometry. If the mixture of products obtained from pyrolysis first can be separated into individual compounds, mass spectrometric identifications are facilitated and analytical reliability increased. A mixture of relatively low molecular weight compounds can be separated by gas chromatography. It should be noted that the term 'chromatography' may be misleading; it is derived from the first separation experiments that involved coloured compounds. In modern usage, chromatography simply defines a separation method regardless of the colour of the separated substances. The technique of directly connected vacuum pyrolysis-gas chromatography-mass spectrometry⁹ provides polymer degradation with minimal secondary (spurious) compound formation and the separation of the components before mass spectrometric analysis.

Usually, capillary column gas chromatography provides the most effective separation (resolution) of complex, volatile mixtures. The stainless steel columns used in the Vaal Reef kerogen study were 46 m long and their internal diameters were 0.5 mm. They were coated inside with a thin layer of an organic substance (stationary phase). The entire mixture of pyrolysis products was injected into the front of the column; the various components were alternately adsorbed on, and desorbed from the stationary

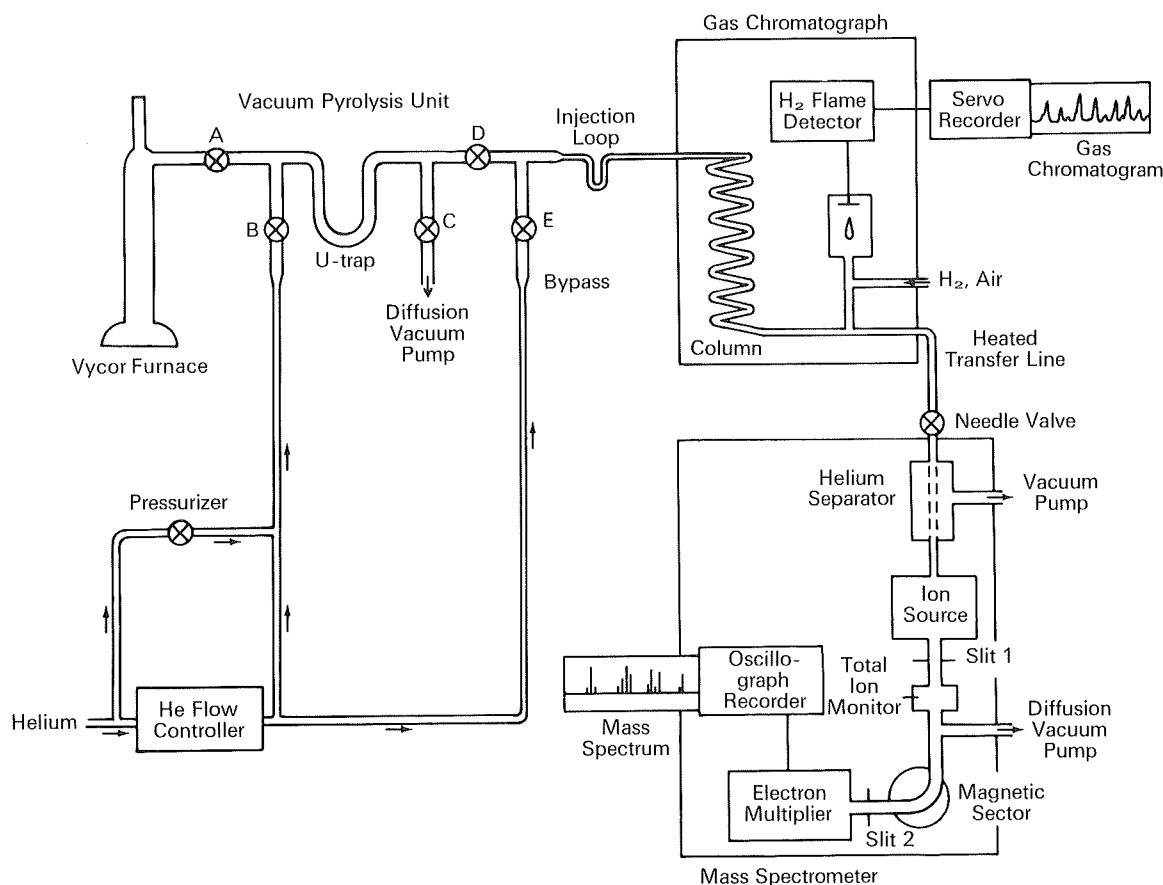


FIGURE 1 Schematic diagram of the combined high-vacuum pyrolysis-gas chromatograph-mass spectrometer system. First, the decontaminated and powdered Vaal Reef kerogen is introduced into the Vycor furnace. Helium flows through the bypass (valve E is open) and into the gas chromatograph. Next, the pyrolysis system is evacuated by opening valves C and A (valves B and D are closed). The furnace is then heated to 100°C to degas the sample and subsequently heated to the pyrolysis temperature (e.g. 450°C). The U-trap is submerged in liquid nitrogen during pyrolysis. The system is next pressurized with He by opening the pressurizer valve after closing valves C and A and opening valve B. Liquid nitrogen is then placed on the small injection loop and the U-trap is heated at 250°C. The transfer of pyrolysis products from the U-trap to the injection loop is accomplished as He flows through valve B and the heated U-trap to the injection loop. Valves C, A, and E are closed and valves B and D are open. After transfer, the injection loop is heated and the pyrolysis products are introduced onto the column in the gas chromatograph as a sharp 'plug'. The needle valve on the heated transfer line (before the He separator) is adjusted so that the separated components from the end of the gas chromatographic column are split between the H₂ flame detector in the gas chromatograph and the ion source of the mass spectrometer. The H₂ flame detector produces a gas chromatogram, and (after He is removed) the ion source in the mass spectrometer bombards the separated compounds with electrons. The mass spectra serve to identify the unknown compounds.

phase at different rates depending upon their volatility, polarity, etc., and consequently emerged from the end of the column at different time intervals. An inert carrier gas, in this case helium, was passed through the columns (usually at rates between 2 and 10 cm³/min) to move the components through the columns; also the columns were heated at uniformly increasing, programmed temperatures. By judicious selection of the appropriate gas chromatographic parameters (i.e., length of column, nature of stationary phase, carrier gas flow rate, temperature programme rate, etc.), the separation of the organic components are optimized. As the individual compounds emerge from the end of the column, they are split into two unequal portions; the smaller one is diverted to a detector. In this case, the compounds were burned in a hydrogen flame detector, which produces a current upon combustion, and subsequently the signals were printed out on a chart as gas chromatographic peaks. Each peak on a well resolved gas chromatogram usually represents a single component with the area under the peak proportional to the quantity of that component. The larger frac-

tion of the compounds emerging from the column is diverted into the organic mass spectrometer for identification. However, before the separated compounds are introduced consecutively into the mass spectrometer, which operates under high vacuum, most of the carrier gas, which is at approximately atmospheric pressure, must be removed. This is accomplished by a system called a molecular separator and by differential pumping. In the organic mass spectrometer, organic compounds are ionized and fragmented by electron bombardment. The resulting parent and fragment ions of the molecule usually bear a +1 charge because of the loss of one electron during electron bombardment. These organic ions are next separated on the basis of their mass-to-charge ratios (m/e) by accelerating the ions through a magnetic field of varying strength in the mass spectrometer. The types and abundances of the ionized fragments of a compound, and often those of the molecular or parent ion, essentially provide a fingerprint pattern. This pattern is recorded and is called the mass spectrum. It then can be compared with mass spectra of known standards of organic compounds

for the purpose of identification. A schematic diagram of the combined vacuum pyrolysis-gas chromatograph-mass spectrometer system is illustrated in Figure 1.

The directly connected vacuum pyrolysis-gas chromatography-mass spectrometry method used in this study has been described previously⁹. Briefly, this technique involves the initial degassing of decontaminated kerogen samples at 100 °C under $\sim 10^{-6}$ torr vacuum for $\frac{1}{2}$ hour. Next, the samples are pyrolyzed at $\sim 10^{-6}$ torr vacuum at a suitable temperature (usually 450 °C) for $\frac{1}{2}$ hour. The pyrolysis products are first collected by condensation under liquid N₂ temperatures. Next the pyrolysis apparatus is pressurized with He, and the products are swept into the capillary gas chromatographic column in a Perkin-Elmer 226 gas chromatograph. The separated components emerging from the gas chromatograph are then introduced into a Hitachi RMU-6E mass spectrometer via a heated transfer line and a Watson-Biemann molecular separator. The resulting mass spectra are identified by comparison with a library of mass spectra of known standards. All Vaal Reef kerogen samples were pyrolyzed at 450 °C after degassing at 100 °C, except for one sample which was pyrolyzed sequentially at 300 °C and 450 °C. The results of these analyses will be described after a discussion of modern biochemical contaminations in the carbon seams in order to facilitate the appraisal of the properties of the syngenetic kerogen.

Contamination controls and sample preparation

The combined gas chromatograph-mass spectrometer is a highly sensitive analytical system. It can detect $\gtrsim 10^{-9}$ grams of an organic compound. Consequently, it is essential that all organic contaminations be removed prior to analysis. Thus, the procedure for preparing sedimentary rocks containing kerogen for pyrolysis as well as other organic analyses must include a step that ensures the removal of non-syngenetic (extraneous) organic matter. The following procedures are used in the authors' laboratory; other investigators use modifications of this process. First, the surfaces of rock samples are drilled off with a high-speed drill to remove weathered material or other possible surface contaminations. Next, the rocks are crushed and thoroughly washed in distilled water in an ultrasonic cleaner to further decontaminate them. After drying, the samples are pulverized to $\gtrsim 200$ mesh in an acid-cleaned ceramic ball mill fitted with a teflon gasket. The powdered samples are then extracted with organic solvents (usually benzene and methanol) to remove soluble, non-kerogen, organic contaminations. All glassware, ceramics, and teflon used during sample preparation and subsequent analyses are acid cleaned with a mixture of hot concentrated H₂SO₄/HNO₃ (85:15, v/v). All organic solvents are freshly redistilled from spectral or pesticide grade reagents. The water is triple distilled in an acid cleaned glass apparatus.

The Vaal Reef samples were prepared for analysis according to this procedure with the exception that the thin kerogen layers were often physically separated from the quartzitic host rocks with solvent cleaned scalpels. The carbonaceous separates are designated in the following discussion, tables, and illustrations by a 'C' following the sample number, and the quartzitic host rock separates by a 'Q'. Samples in which the carbonaceous matter was not separated from the host rock are represented by a 'T' following the sample number.

Blank experiments (i.e., complete experiments without any sample) and controls must be routinely performed to ensure that no laboratory contamination occurred. During blank experiments, acid-cleaned empty pyrolysis chambers were heated under vacuum at temperatures identical to those in which the carbon-rich Vaal Reef samples were pyrolyzed to ensure that the gas chromatographic traces and mass spectra showed no extraneous organic compounds. These steps are necessary because even amino acids from a single fingerprint on laboratory glassware may lead to erroneous results.

Other organic contaminations may arise from interstitial water permeating through sedimentary rocks after the kerogen developed and before the samples reached the laboratory. Several investigators have shown^{10,11,12,13} that even dense rocks, such as cherts, not to mention the more porous and permeable carbonaceous material, can and are easily contaminated with soluble organic matter introduced by aqueous solutions after deposition. Also, in most mining operations there is sufficient water, and virtually every organic substance present (petroleum products from machinery and biochemicals from human contact) can pose as a serious source of contamination. To evaluate this possible source of contamination in the Vaal Reef kerogen, water samples used in mining operations were analysed for modern organic matter. Approximately 10 ml of water collected in the Welkom Gold Mine was evaporated to dryness under a stream of nitrogen purified by an appropriate filter. In the mine, this water sample flowed down a stope face and ran down a slusher gully in which a scraper was operating. After evaporation, 70 mg residue remained from the 10 ml mine water sample. The residue was degassed at room temperature under 10^{-6} torr vacuum and subsequently pyrolyzed at 450 °C. This procedure was selected to simulate the analytical processes used for the carbonaceous Vaal Reef samples. The pyrolysis products from the mine water residue were separated by gas chromatography and identified by mass spectrometry.

The mine water was also analysed by three additional techniques. In the first experiment one ml of mine water was placed on a Whatman No. 2 filter paper and allowed to dry. An 0.2 per cent ninhydrin solution in alcohol was finely sprayed on the filter paper, which was subsequently heated at 100 °C for one hour. The ninhydrin reaction is a classical and highly sensitive method for identifying amino acids. Two other filter papers were used as controls; one contained 1 ml of mine water but no ninhydrin reagent and the other one was treated only with ninhydrin but contained no mine water.

In the second experiment contamination of the Vaal Reef kerogen by mine water was assessed by an examination of the relative age of the amino acids extracted from the carbon seam. It is possible to do this age determination because, like quartz, amino acid molecules occur in both left- and right-handed configurations, called L- and D-enantiomers. However, unlike quartz, most amino acids in living organisms occur only in the left-handed configuration. However, upon the death of an organism they slowly change to an equal mixture of L- and D-enantiomers; this process is called racemization. A powdered Vaal Reef kerogen sample was extracted with 100 ml of boiling distilled water for two hours to extract amino acids, and then the solution was removed by filtration. The following procedures enabled the separation of L- and

D-amino acids by gas chromatography. The filtrate was first evaporated to dryness and the residue was redissolved in 0,06 N HCl. This solution was placed on a cation exchange column to remove inorganic salts; the amino acids that remained on the column were subsequently washed from the column with 1 N NH₄OH, which then was evaporated to dryness. Anhydrous acidified + -2-butanol (2-4 N; purity: 99 per cent) was added to the residue and heated at 100°C for three hours to esterify the carboxylic functional groups of the amino acids. Next, to make the amino acid derivatives sufficiently volatile for gas chromatography, the solution was evaporated and 2 ml of CH₂Cl₂ together with 0,2 ml of pentafluoropropionic anhydride was added to the amino acid ester residue. This reaction acylated the amine functional group of the amino acids. The resulting amino acid enantiomeric derivatives were separated on a Perkin-Elmer F-11 gas chromatograph using a Carbowax 20 M capillary column (46 m × 0,5 mm) and the relative abundances of the L- and D-enantiomers were determined.

In the third experiment, 1 ml of a 5 per cent aqueous phenol solution was added to 1 ml of mine water and again to another test tube that contained 1 ml of distilled water (control). Five ml of concentrated sulphuric acid was then added to each test tube. The phenol-sulphuric acid colour reaction is a sensitive and classical method used for the identification of carbohydrates. The absorption of these solutions were measured at 490 m μ (visible spectral region) on a Bausch & Lomb Spectronic 20 spectrophotometer.

The results of the mass spectrometric analyses of the mine water residue pyrolyzates showed the presence of various organic compounds. Significant components identified from the residue included furan, acetaldehyde, ethanenitrile, acrylonitrile, and benzonitrile. It has been noted¹⁴ that the first two of these compounds are common pyrolysis products of carbohydrates, and that the latter three are pyrolysis products of amino acids and/or other nitrogenous compounds. Petroleum products (such as used in various mine machinery) were virtually absent in the mine water residue, with the exception of a C₃-alkylbenzene. This is surprising because petroleum products are abundant contaminations in the mines, as was observed by one of the authors (B. N.).

The results of the three additional experiments on the mine water also showed that the Vaal Reef kerogen samples are contaminated with modern soluble organic matter. Mine water analyses gave positive amino acid and carbohydrate reactions. The ninhydrin reaction showed the characteristic purple colour on the filter paper to which mine water was added. The two filter papers which served as controls showed negative colour reactions. After the phenol-sulphuric acid test the mine water showed the characteristic yellow colour with the 490 m μ absorption maximum, yielding evidence for the presence of sugars and starches. In the control experiment, which consisted of the analysis of distilled water only, no colour developed when phenol and sulphuric acid were added to the water in the test tube. This control experiment and the two performed concurrently with the ninhydrin test show that the colour reactions with the mine water were real. Thus, the mine water contains amino acids as well as sugars and starches.

Two amino acids (aspartic acid and proline) in the hot water extract of the kerogen were identified by gas chromatography; they consisted of the L-enantiomer only; neither of their D-enantiomers were present in significant amounts.

This means that these amino acids did not even have time to begin to racemize; thus, they are modern contaminations. If these two amino acids were syngenetic to the Vaal Reef samples and had survived the rigours of 2 500 million years of geologic time, then most probably they would exist as racemic mixtures; i.e., they would consist of a mixture of 50 per cent L-aspartic acid and 50 per cent D-aspartic acid, etc. It is well documented^{10,15} that upon the death of an organism, amino acids begin to racemize from their L-configuration in the living organism to their D-counterparts at rapid rates in the geological time scale. Aspartic acid is one of the amino acids that racemizes most rapidly. It is conceivable that clays in the rock and kerogen could have retarded the racemization reaction¹⁶. On the other hand, certain bacterial cell components contain D-enantiomers of amino acids and the progenitor of the kerogen was a blue-green algal/bacterial mat. These are the considerations that led to the conclusion that the presence of L-amino acids in the kerogen represents modern contaminations.

Mine waters must have introduced modern amino acids and carbohydrates into the Vaal Reef carbon seams. This could lead to the misinterpretation of the results of the analyses of the Vaal Reef kerogen because modern contaminations may be mistaken for syngenetic components. The effect of such an error on the evaluation of the composition, structure, and particularly of the origin and evolution of the carbon seams, would be considerably distracting. This is why the Vaal Reef kerogen was decontaminated prior to analyses by repeated solvent extractions. Consequently, and as will be noted below, furan, acrylonitrile, or ethanenitrile have not been identified in the solvent-cleaned Vaal Reef samples analysed by vacuum pyrolysis-gas chromatography-mass spectrometry.

Results of the Vaal Reef kerogen pyrolysis

Seventeen decontaminated samples of Vaal Reef kerogen were analysed by high vacuum pyrolysis-gas chromatography-mass spectrometry. These samples, from the Klerksdorp area, were collected in the Stilfontein Gold Mine (Nos SVR-15C, SVR-202C, SVR-235C, and SVR-260C); the Hartebeestfontein Gold Mine (No HVR-1C); the Buffelsfontein Gold Mine (Nos BVR-33C and BVR-46C); the Vaal Reef Mine (Nos VVR-6C, VVR-8C, VVR-21C, VVR-31C, and VVR-35C); and the Western Reefs Mine (Nos WVR-2C, WVR-10C, WVR-30C, WVR-32C, and WVR-45C). In the sample designations, the first letter represents the mine; the second and third letters represent Vaal Reef; the numbers refer to sample locations; and C denotes kerogen separated from the host rock.

Gas chromatograms of the 450 °C pyrolysis products of two different samples (SVR-202C and WVR-45C) are shown in Figures 2 and 3, respectively. These chromatograms show all compounds emerging from the column after benzene. For the clarity of these illustrations, the first compounds emerging from the column, including benzene, are not shown on these complex gas chromatograms; they are illustrated separately (Figure 4) for easier viewing. All samples that were pyrolyzed generally consist of the same major components although the relative abundances vary. The mass spectral identifications of the major components of the Vaal Reef kerogen are listed in Tables 1 and 2 together with their gas chromatographic peak numbers corresponding to Figures 2, 3, and 4. It should be added that a few of the aromatic isomers such

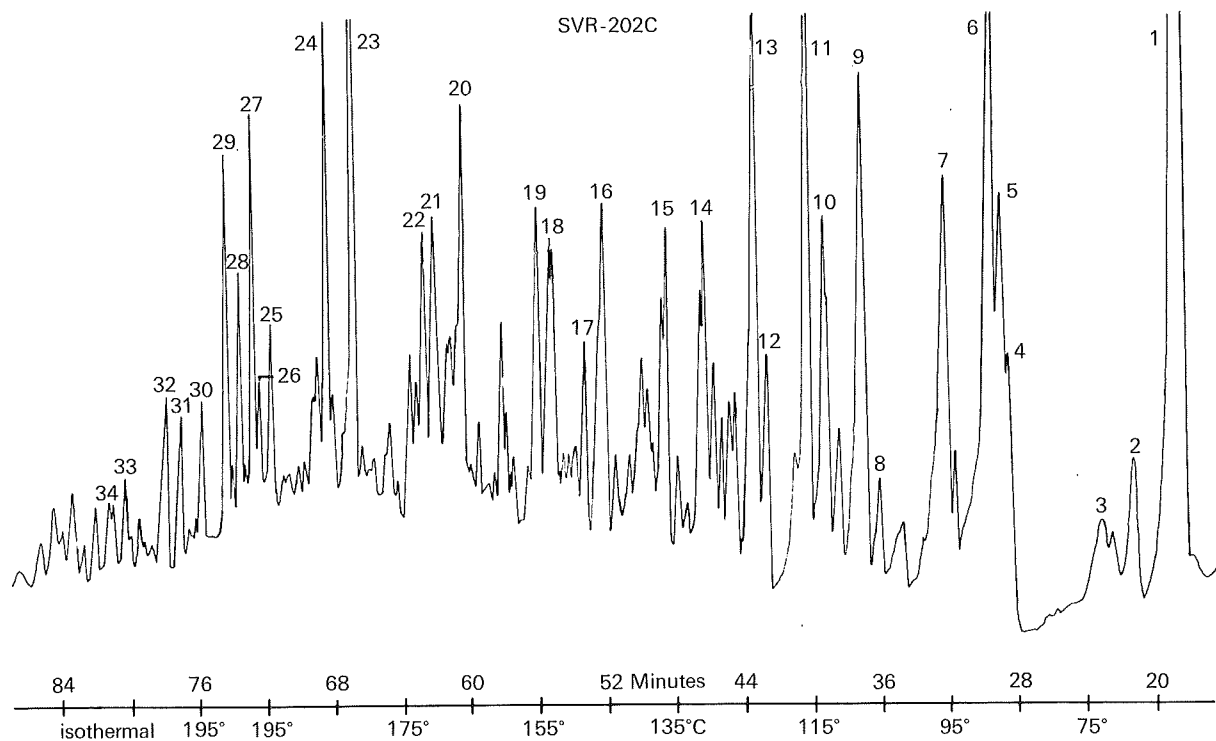


FIGURE 2 Gas chromatogram of the 450°C pyrolysis products emerging from the column after benzene. Sample: SVR-202C (see text for sample designation) after it was extracted with solvents and degassed at 100°C. Polyphenyl ether support coated, open tubular column: 0.5 mm × 46 m.

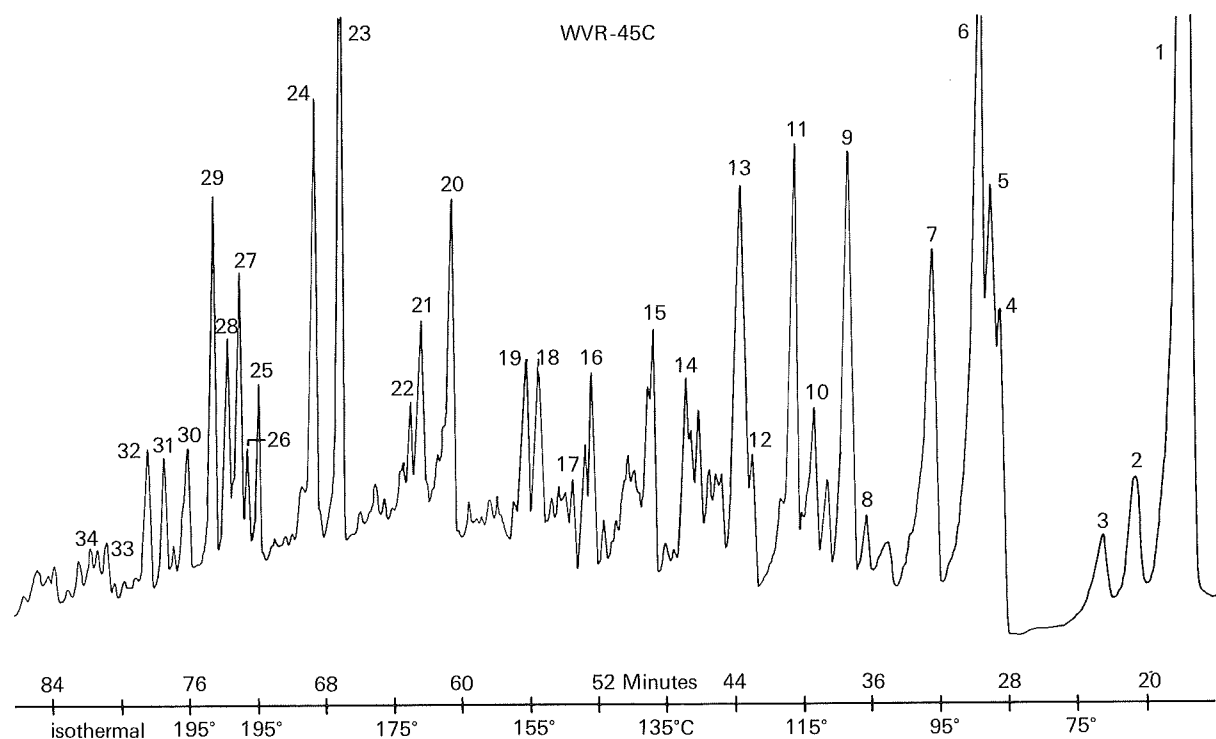


FIGURE 3 Gas chromatogram of the 450°C pyrolysis products emerging from the column after benzene. Sample: WVR-45C after solvent extraction and degassing at 100°C. Polyphenyl ether support coated, open tubular column: 0.5 mm × 46 m.

as dimethylbenzenes, (i.e., *p*, *m*, *o*-xylenes) etc., have virtually indistinguishable mass spectra under applicable analytical conditions but can be identified on the basis of relative retention times, that is, the respective periods of time required by these isomers to pass through the gas chromatographic column. Alkyl substituted aromatic components and low molecular weight aliphatic hydrocarbons along with a few aromatic sulphur compounds comprised the majority of the pyrolysis products. Nitrogen containing compounds have not been detected, but three organic oxygen compounds (acetaldehyde, methanol, and occasionally acetone) were present in low concentrations.

The capillary gas chromatographic column used in these analyses was coated inside with polyphenyl ether. It is known from other pyrolysis experiments conducted in this laboratory^{6,17} that this column is effective in separating a variety of biologically significant pyrolysis breakdown products including several nitrogen- and oxygen-containing organic compounds such as furan, furaldehyde, alkyl, and aromatic nitriles, as well as aromatic and aliphatic hydrocarbons and organic sulphur compounds. Therefore, volatile nitrogen compounds, which usually are detected in Precambrian kerogens, also should have been detected in the Vaal Reef kerogen had they been present. Two facts need to be considered in connexion with these results. First, elemental analyses of two samples (VVR-31C and SVR-260C) showed 600 p.p.m. and 900 p.p.m. organic nitrogen, respectively. Second, polar macromolecules will not pass through capillary gas chromato-

TABLE 1
MASS SPECTRAL IDENTIFICATIONS OF THE MAJOR GAS CHROMATOGRAPHIC PEAKS SHOWN IN FIGS. 2 AND 3;
450°C PYROLYSIS

Gas Chromatographic Peak Nos. (corresponding to Figs. 2 and 3)	Compound
1	toluene
2	2-methylthiophene
3	3-methylthiophene
4	ethylbenzene
5	<i>p</i> -xylene
6	<i>m</i> -xylene
7	<i>o</i> -xylene
8	<i>n</i> -propylbenzene
9	methylmethylenbenzene
10	methylmethylenbenzene
11	trimethylbenzene
12	methylstyrene
13	methylpropylbenzene
14	C ₄ -benzene
15	indene
16	methylindane
17	methylindane
18	methylindene
19	methylindene
20	naphthalene
21	benzothiophene
22	methyl-1, 2-dihydronaphthalene
23	2-methylnaphthalene
24	1-methylnaphthalene
25	ethylnaphthalene
26	ethylnaphthalene
27	dimethylnaphthalene
28	dimethylnaphthalene
29	dimethylnaphthalene
30	dimethylnaphthalene
31	dimethylnaphthalene
32	propylnaphthalene
33	trimethylnaphthalene
34	trimethylnaphthalene

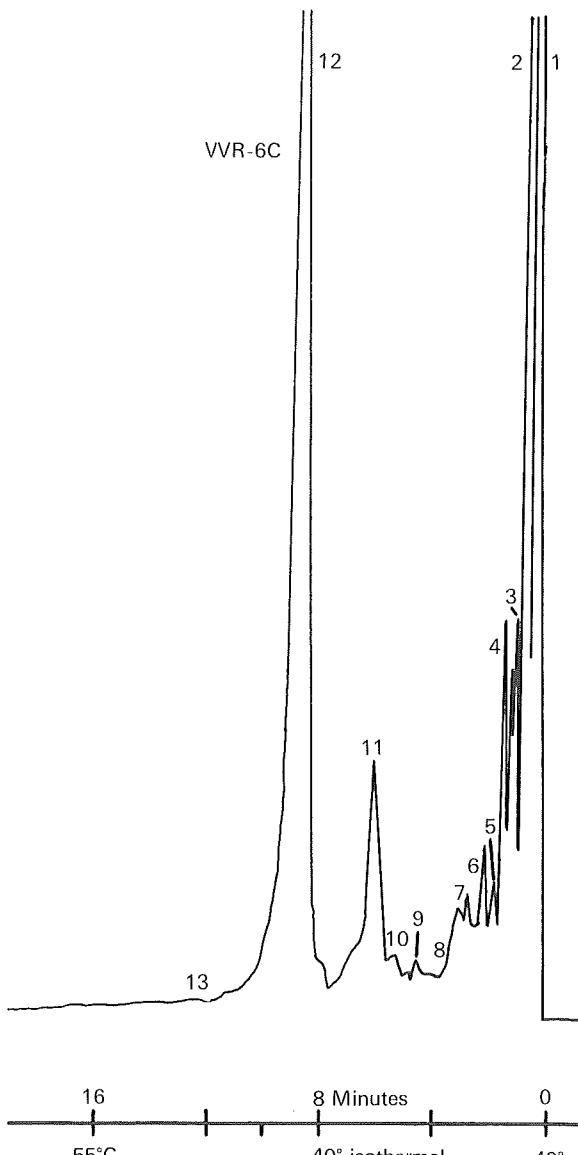


FIGURE 4 Typical gas chromatogram of the low molecular weight 450°C pyrolysis products emerging from the column before toluene. Sample: VVR-6C after it was extracted with solvents and degassed at 100°C. Same column as in Figures 2 and 3.

graphic columns. These facts suggest that traces of nitrogenous components in the Vaal Reef kerogen apparently are held far more tightly in the polymer matrix than in the matrices of ordinary Precambrian kerogens, and consequently they did not fragment during pyrolysis into the low enough molecular weight constituents that are amenable to analysis.

Figures 5 and 6 show gas chromatograms of sequential pyrolyses at 300°C and 450°C, respectively, of sample VVR-35C. Table 3 lists the corresponding 300°C pyrolysis products. Figures 5 and 6 illustrate that the higher molecular weight components of the Vaal Reef kerogen are not broken down from the random polymer until 450°C, even with prior heating at 300°C. Minor components obtained from the pyrolysis experiments from all samples, (i.e., those compounds not shown in Tables 1 to 3) are listed in Table 4.

TABLE 2
MASS SPECTRAL IDENTIFICATIONS OF GAS CHROMATOGRAPHIC PEAKS SHOWN IN FIGURE 4;
450°C PYROLYSIS

Gas Chromatographic Peak Nos. (corresponding to Figure 4)	Compound
1	ethane, ethene
2	propane, propene, COS
3	butane, butene
4	pentane, SO ₂
5	dimethylcyclopropane
6	methanethiol, dimethyldisulphide (minor)
7	pentadiene
8	methylpentene
9	CS ₂
10	hexadiene, dimethylsulphide (minor)
11	acetaldehyde
12	methanol, heptadiene (minor)
13	benzene
	thiophene

TABLE 3
MASS SPECTRAL IDENTIFICATIONS OF GAS CHROMATOGRAPHIC PEAKS OF SAMPLE VVR-35C (FIG. 5), 300°C PYROLYSIS

Gas Chromatographic Peak Nos. (corresponding to Figure 5)	Compound
1	CO ₂ , ethane, ethene
2	<i>n</i> -butane, COS
3	SO ₂
4	methylbutene
5	methylpentene
6	hexane
7	hexene
8	dimethylsulphide, CS ₂
9	acetaldehyde
10	methanol, methylethylsulphide (minor)
11	benzene
12	toluene

Electron paramagnetic resonance spectroscopy

This method is used to determine the quantity of free radicals in a sample. A free radical is an atom or a molecule containing an unpaired electron. The free radical content of organic substances is the result of various processes; one major cause is irradiation from radio-active elements. Normally, free radicals are highly reactive, especially in solutions where they rapidly combine with each other. Because of this reason, free radical reactions are utilized in making a number of synthetic polymers, such as certain plastics. However, in many types of solid organic matter, such as coal, free radicals are relatively stable. Organic free radicals can be detected by using electron paramagnetic resonance (sometimes also referred to as electron spin resonance) spectroscopy. The odd spin of the unpaired electron in a free radical generates a magnetic field or moment that reveals itself as two distinct energy levels in an external magnetic field. (The two opposite spins in the usual paired electrons cancel out each other.) The energy difference between the unpaired electron's two possible orientations in an external magnetic field can be detected by the application of electromagnetic radiation of a specific frequency that is absorbed during electronic transitions between the two energy levels. At magnetic field strengths of approximately 3 400 gauss, the absorption frequency (energy) of free electrons falls in the microwave region of the electro-magnetic spectrum.

Three powdered Vaal Reef samples (WVR-30C, WVR-32C, and WVR-45C) were analysed by electron paramagnetic resonance spectroscopy (EPR) with a Varian E-3 spectrometer at room temperature to determine their free radical content. The microwave and modulation frequencies were set at 9,493 GHz and 100 Hz, respectively, the magnetic field was 3 380 gauss, and the scan range was ± 10 gauss. The scan range was expanded when looking for inorganic free radicals in the kerogen.

The results of the EPR spectroscopy are listed in Table 5. All three samples studied yielded unusually high concentrations of spins or free radicals per gram of kerogen carbon. Figures 7 and 8 show the EPR spectra of the three samples. The area under the curves corresponds to the quantity of organic free radicals in the sample when it is compared with the area under the curve of a standard of known free radical concentration. The width of the curve is generally a function of the types of free radicals present. A parameter known as the g value is also characteristic of the type of free radicals present. The Vaal Reef kerogen g value (2.0067) is close to the free electron spin value (2.0023) and is consistent with delocalized unpaired

TABLE 4
MINOR PYROLYSIS COMPONENTS IDENTIFIED BY GAS CHROMATOGRAPHY-MASS SPECTROMETRY

Aliphatic Hydrocarbons	Aromatic Hydrocarbons	Organic Sulphur Compounds
methylpropene	dimethylethylbenzenes	ethanethiol
pentene	C ₅ -alkylbenzenes	ethylthiophenes
methylpentane	C ₆ -alkylbenzenes	dimethylthiophene
methylcyclopentene	styrene	C ₃ -alkylthiophene
methylhexene	indane	C ₄ -alkylthiophene
C ₇ -alkane	C ₂ -alkylindanes	methylbenzothiophene
C ₁₀ -alkane	C ₃ -alkylindanes	C ₂ -alkylbenzothiophene
	C ₄ -alkylnaphthalenes	C ₃ -alkylbenzothiophene
	acenaphthene	dibenzothiophene
		thiophenothiophene

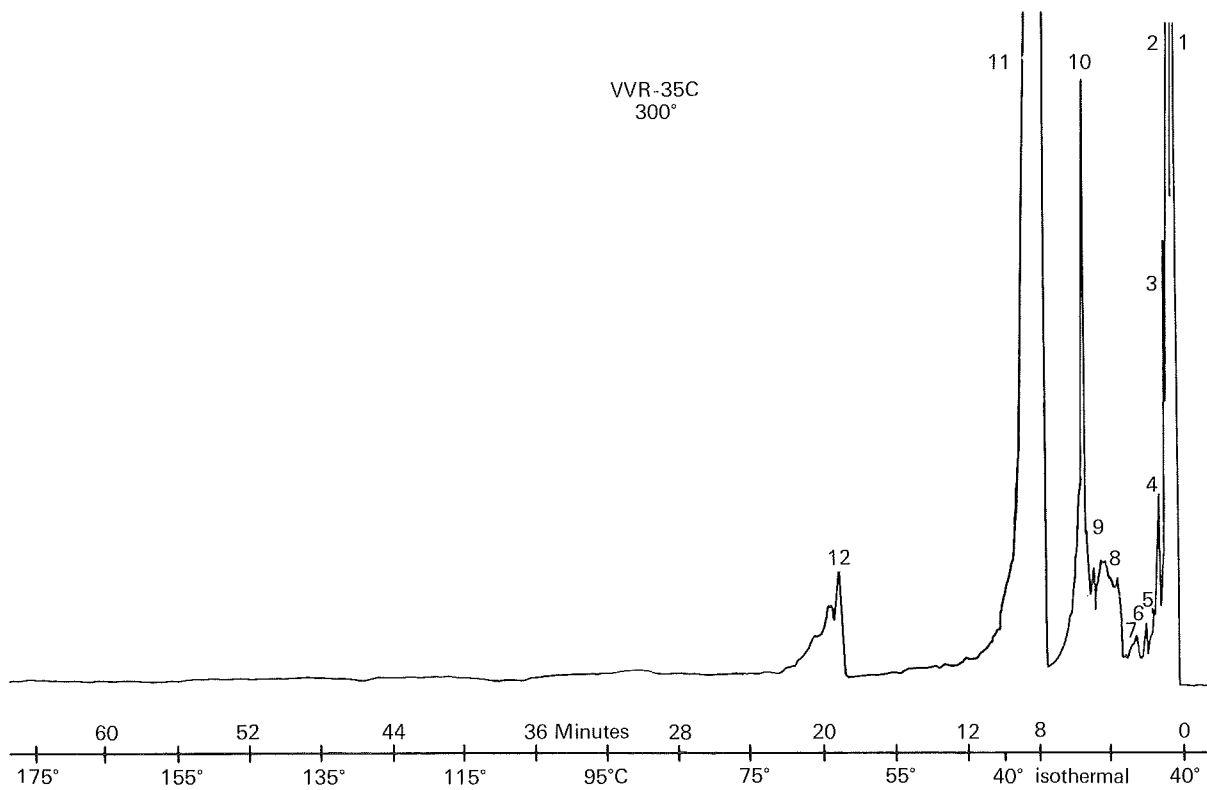


FIGURE 5 Gas chromatogram of the 300°C pyrolysis products of sample VVR-35C after solvent extraction and degassing at 100°C. Same column as in Figures 2 and 3.

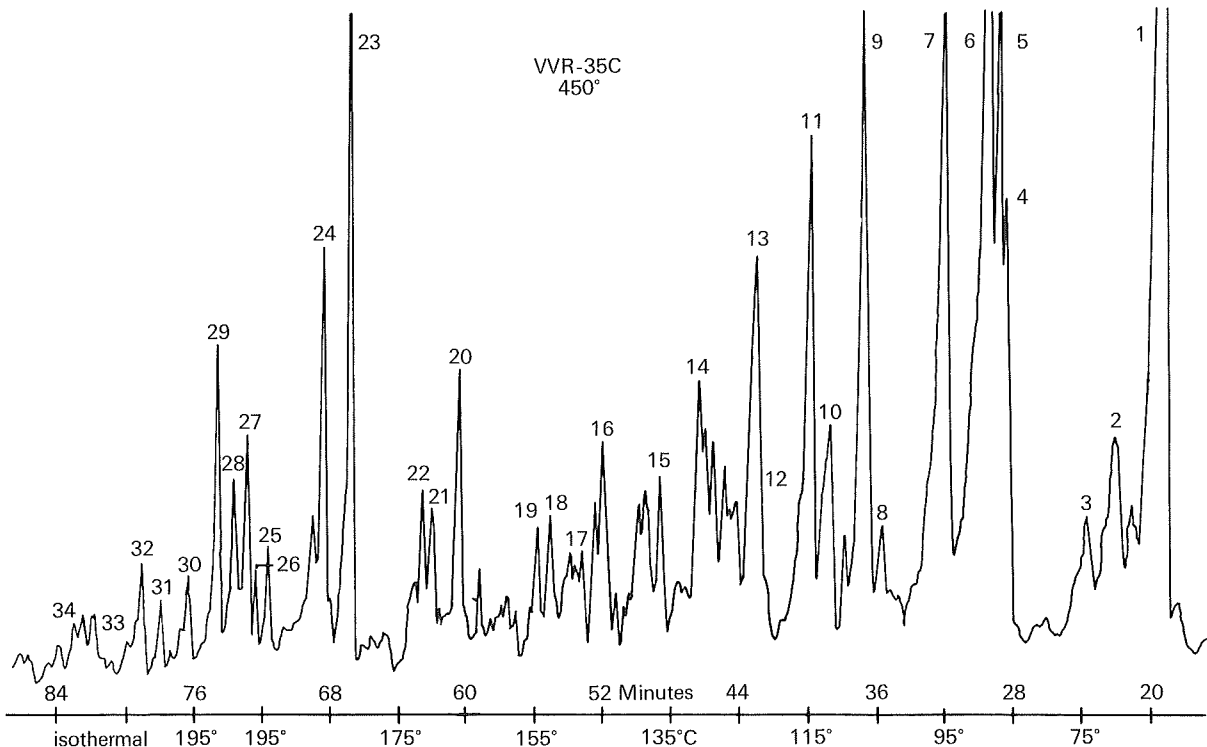


FIGURE 6 Gas chromatogram of the 450°C pyrolysis products of sample VVR-35C after prior pyrolysis at 300°C. Same column as in Figures 2 and 3.

TABLE 5
ELECTRON PARAMAGNETIC RESONANCE (EPR) SPECTROSCOPY* OF VAAL REEF KEROGEN SAMPLES
WVR-30C, WVR-32C, and WVR-45C

	Standard (DPPH)†	WVR-30C	WVR-32C	WVR-45C
width (gauss)	1.8	4.1	3.5	2.8
height (h)	79.5	63	30	63
area = h × width ²	257.6	1059.0	367.5	493.9
gain	1.25×10^2	3.2×10^2	1.25×10^2	1.25×10^2
weight (grams)	0.0087	0.2831	0.2322	0.1954
fraction carbon	—	0.220	0.199	0.232
spins/g carbon†	—	3.4×10^{20}	4.0×10^{20}	5.5×10^{20}

*Microwave Frequency = 9,493 GHz; Modulation Frequency = 100 Hz; Field Set = 3380 Gauss; Scan Range = $\pm 1 \times 10$ Gauss; Temperature = 25 °C

†Diphenylpicrylhydrazyl, molecular weight = 394

0.0087 g = 2.2×10^{-6} moles DPPH

Assuming 100% free radicals: (2.2×10^{-6} moles) (6.03×10^{23} spins/mole) = 1.3×10^{19} spins

$$\text{spins/g carbon in kerogen} = 1.3 \times 10^{19} \times \frac{\text{area sample}}{\text{area DPPH}} \times \frac{\text{gain DPPH}}{\text{gain sample}} \times \frac{1}{\text{sample weight}} \times \frac{1}{\text{elemental carbon fraction}}$$

electron spins in aromatic organic systems and inconsistent with minerals. One sample showed an additional but very small absorption effect (removed on the scale from the large curve which is the result of the organic free radicals). This small absorption effect probably is caused by unpaired electrons in some metallic atoms of minerals.

Carbon-hydrogen atomic ratios

A simple and commonly used parameter in organic geochemistry, coal chemistry, etc., is the carbon-hydrogen atomic ratios (C/H) of the organic matter. These ratios were determined in the Vaal Reef kerogen samples. Next, these ratios were compared to the C/H ratios of unaltered biochemicals, various ranks of coal, humic acid, petroleum asphaltenes, etc.^{18,19,20,21,22}. It needs to be noted that the C/H ratios are of somewhat limited utility in elucidating the nature of organic substances, yet they can be useful in defining certain general properties. For example, the simplest aromatic hydrocarbon, benzene (C_6H_6), has a C/H ratio of 1.00, and graphite, which consists of a series of conjugated, π -bonded, six-membered carbon rings arranged in sheets and containing no hydrogen, has a C/H ratio of infinity. Highly aromatic substances, coals and metamorphosed anthracites have C/H ratios between the values of benzene and graphite. The common and unaltered biochemicals, which are believed to have been present in micro-organisms prevalent during the Precambrian, fall below C/H = 1.00 because they are basically non-aromatic in nature. These biochemicals exclude the lignin of the more highly evolved plants that first arose during the Paleozoic Era. The biochemicals of interest in the context of this study consist mainly of carbohydrates,

lipids, proteins, and nucleic acids. The C/H atomic ratios of various organic substances and Vaal Reef kerogen samples are shown in Figure 9. It is apparent from this diagram that the majority of the Vaal Reef kerogen falls into the petroleum asphaltene to low rank anthracite C/H range. This comparison is not intended to imply that there is any genetic relation between coal, petroleum, and the Vaal Reef kerogen.

The Vaal Reef C/H ratios were plotted against X-ray abundance functions of three minerals, the 7.05 Å clay, 3.34 Å quartz, and 2.71 Å pyrite X-ray diffractometer peak areas. It should be noted that the respective peak areas approximate, but do not necessarily represent, the exact amounts of these three minerals disseminated in the kerogen. This correlation between C/H ratios and mineral abundance functions was performed because it is conceivable that some relation between the C/H ratios and the major mineral components of the Vaal Reef kerogen may reveal genetic and diagenetic trends. It should be noted in connexion with these studies that after preliminary X-ray diffraction analysis some of the Vaal Reef kerogen samples were treated with HF to remove quartz, whose major X-ray reflexion overlaps the main graphite (002) peak²³. The HF treated samples were analysed again by X-ray diffraction. No graphite was found in Vaal Reef kerogen samples. A few C/H ratios, including those of the quartzite host rocks adjacent to the auriferous organic cores, have zero (no carbon present) or significantly low values and fall below the unaltered biochemicals. Excess hydrogen from clay minerals could account for these values.

The straight line in Figure 9 represents the least square best fit relation between C/H and per cent clay. The two

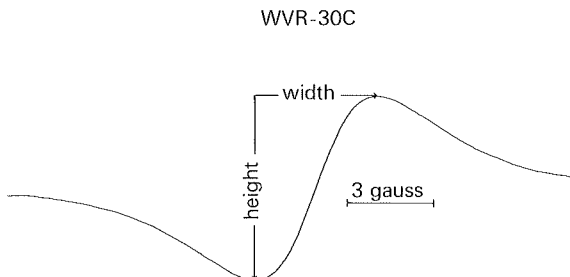


FIGURE 7 Electron paramagnetic resonance spectrum of sample WVR-30C. Microwave frequency = 9,493 GHz; modulation frequency = 100 Hz; field set = 3380 gauss, scan range = ± 10 gauss; temperature = 25 °C. Gain 3.2×10^2 .

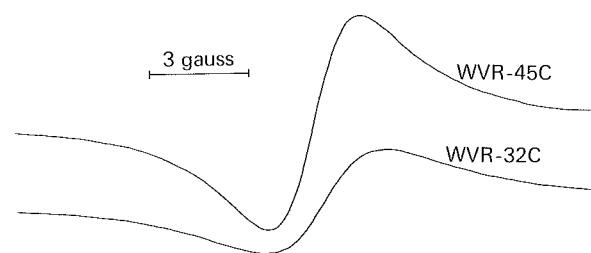


FIGURE 8 Electron paramagnetic resonance spectra of samples WVR-32C and WVR-45C. Spectrometer conditions same as in Figure 7, except gain = 1.25×10^2 .

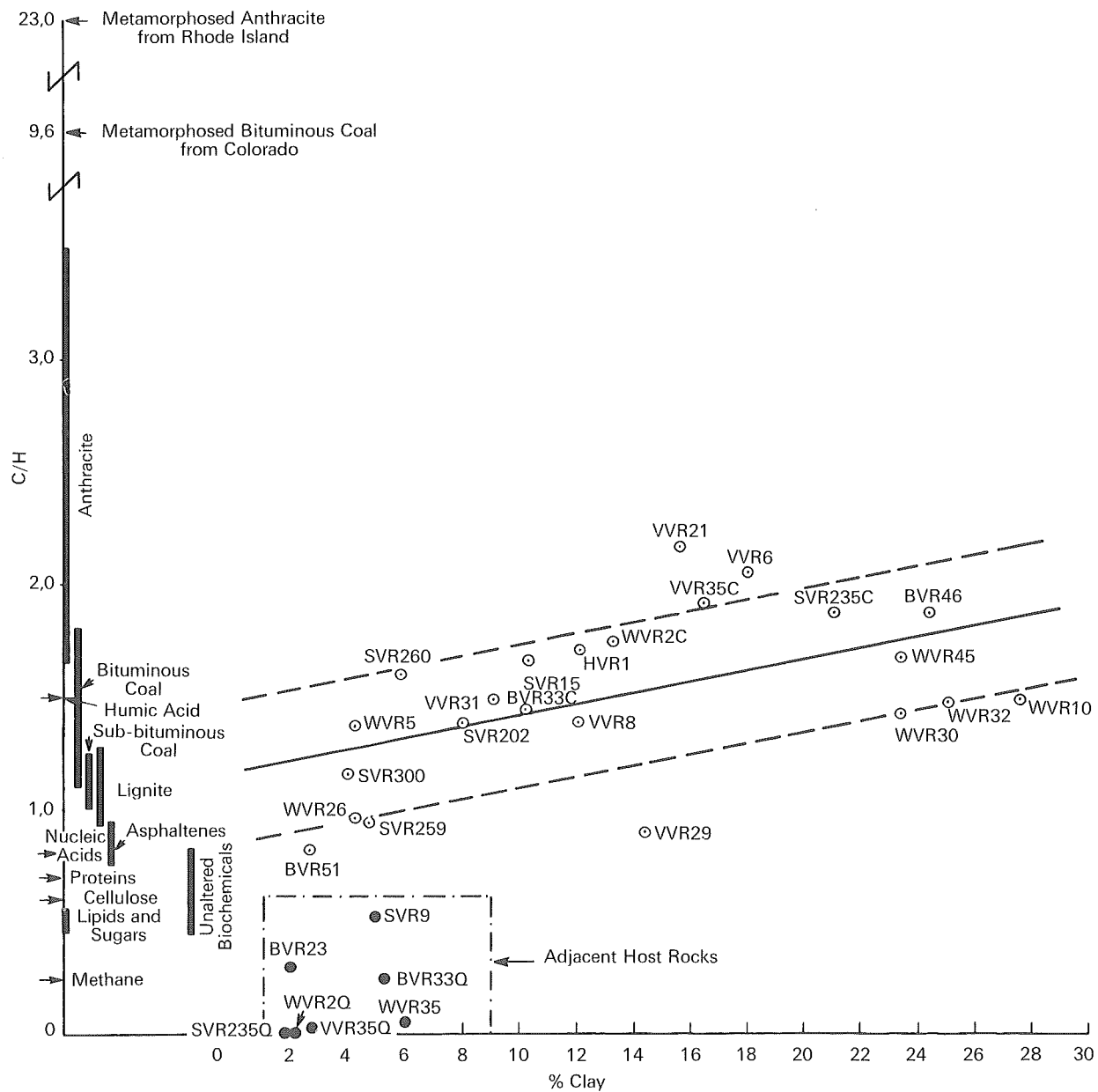


FIGURE 9 Correlation between C/H atomic ratios and clay content determined from X-ray diffractometer peak areas[(clay/quartz + pyrite + clay) \times 100] of Vaal Reef samples. Characteristic C/H ratios of various organic substances are shown on the vertical axis. Note that the majority of the Vaal Reef organic matter have C/H ratios that fall above unaltered biochemicals but far below metamorphosed bituminous coal and anthracite. The straight line spanning the diagram is the calculated least square best fit, and the two parallel dashed lines define the standard error of estimate.

parallel dashed lines represent another statistical parameter, the standard error of estimate. The relatively low correlation between C/H ratios and clay content indicates that the quantity of clay is one, but certainly not the only factor affecting the kerogen carbon-hydrogen atomic ratios. Heat, pressure, and radiation over long periods of time also affect the C/H atomic ratios.

Scanning electron microscopy and electron microprobe analyses

Surfaces of samples can be examined at high magnifications by scanning electron microscopy. The elemental composition (for most elements) of as small as $\sim 1 \mu\text{m}^2$ areas on the surfaces of samples can be quantitatively

determined by the electron microprobe. A combined scanning electron microscope-electron microprobe (ARL Scanning Electron Microprobe Quantometer) was used to determine elemental distributions (including carbon) and the corresponding surface morphologies of freshly broken, unpolished Vaal Reef kerogen. This single instrument was designed to serve dual functions; scanning electron microscopy and electron microprobe analyses (energy dispersive spectra is also a feature of this instrument). By changing the basic parameters of the electron optics, the scanning electron microscope performs as a regular electron microprobe; its detection limit for carbon is ~ 250 p.p.m.

After scanning electron microscopic examinations, selected areas of Vaal Reef kerogen were mapped (scanned),

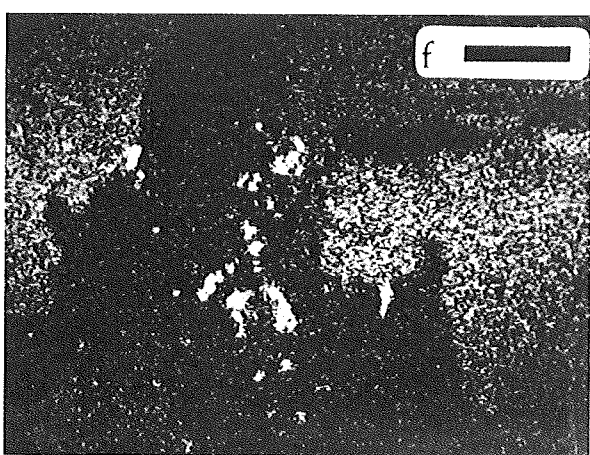
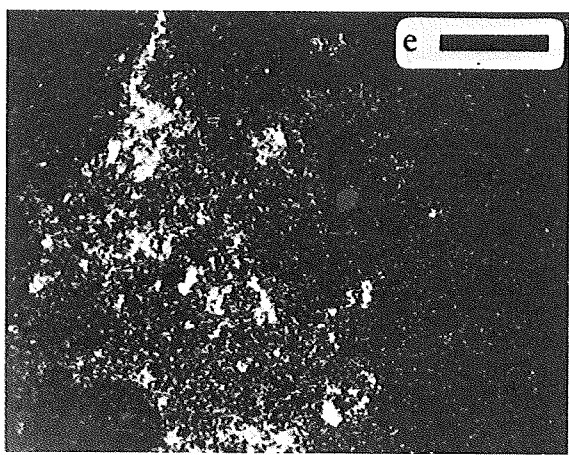
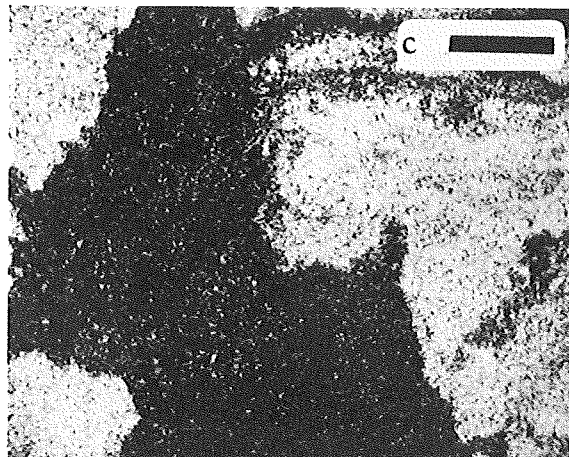
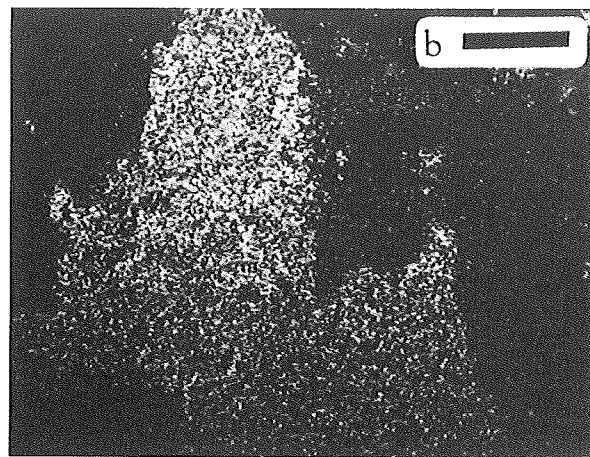
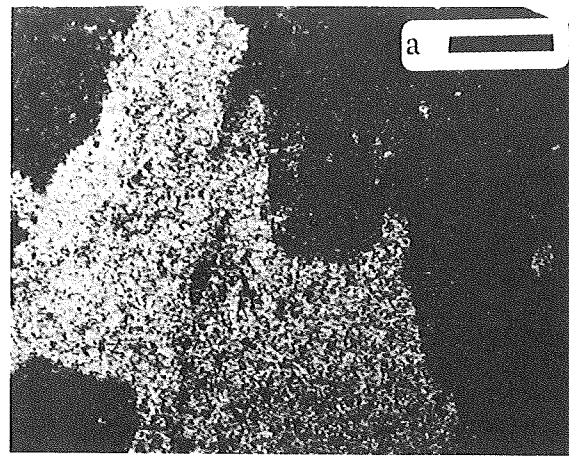


FIGURE 10 Electron microprobe images of a selected area on a freshly broken, unpolished surface of sample WR-31C from the Vaal Reef carbon seams. Light areas represent high concentrations of the following elements; (a) silicon, (b) aluminium, (c) carbon, (d) gold, (e) iron, and (f) sulphur. Magnesium was not detected. Note the irregular, angular shape of the Si, Al, and Fe region, suggesting clay deposition in voids in the organic matter. The horizontal dark lines represent 100 μ m.

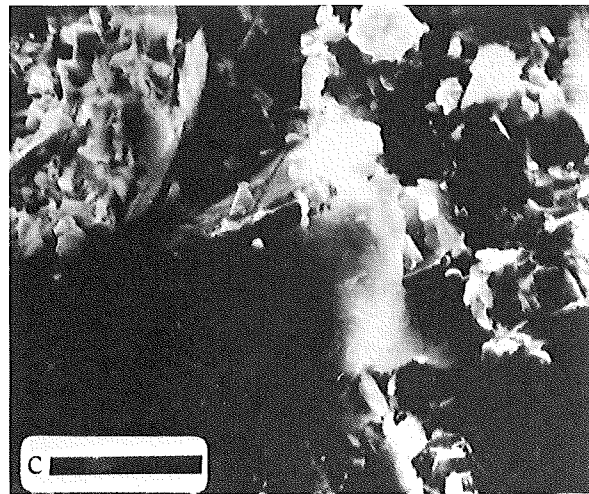
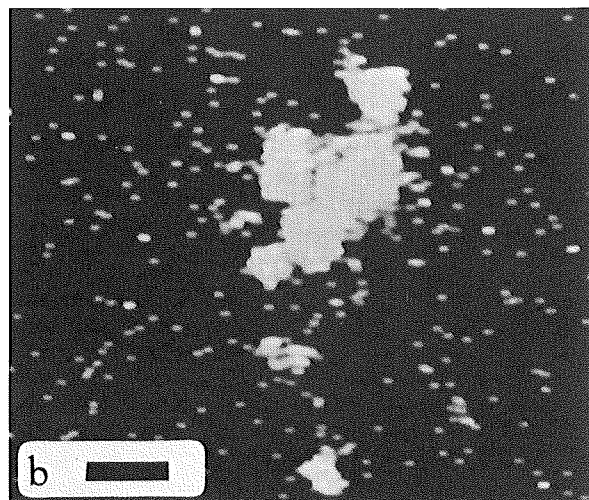
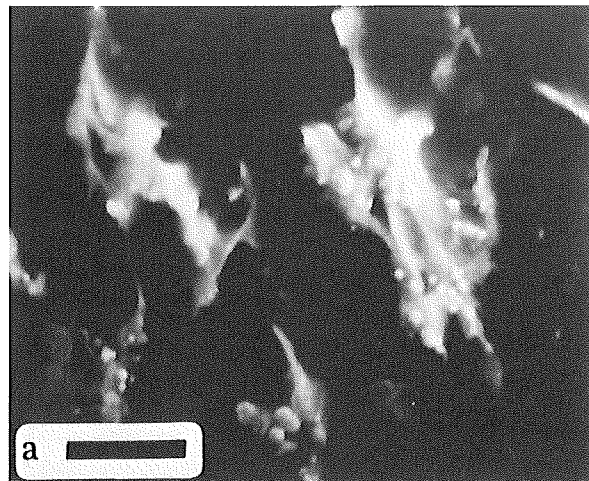
at various magnifications, with the electron microprobe for the following elements: Si, Al, Mg, Fe, S, C, and N. Some of the resulting photographs of the elemental distributions are shown in Figures 10, 11, and 12. Light areas represent enrichment in the specified element.

The results of the electron microprobe analyses showed that the carbon seams consisted of two finely admixed substances of different chemical compositions. One of the components contained mainly Si, Al, and Fe together with subordinate amounts of sulphur and gold; S was associated with Fe. Scanning electron micrographs of this component showed the presence of flaky minerals (Figure 11c). Clay minerals were confirmed to be the major components of this substance by X-ray diffraction analyses. X-ray diffraction indicated that the prominent 7.05 Å basal reflexion was probably caused by a sepiitechlorite clay mineral. The other component detected by electron microprobe analyses consisted basically of an organic substance (i.e., the kerogen) containing (non-pyrite) sulphur and occasionally nitrogen in addition to carbon. No magnesium was detected in either of the components that were examined.

Gold frequently occurred adjacent to clay-kerogen boundaries in both the clay and organic phases. A gold particle associated with clay is shown by the arrow in Figure 10d, and photographically enlarged in Figure 11b. The apparent rectangular shape (which can be either an octahedron with its 001 crystallographic axis aligned with the electron beam, or a cube) of this grain of gold is likely the result of the (re)crystallization of dissolved/colloidal gold. However, the great majority of gold particles showed detrital morphology.

The corresponding scanning electron micrograph, Figure 11c, does not show any rectangular minerals; it shows flaky, clay particles. The rectangular gold structures are apparently buried below the surface of the sample. The electron beam of the microprobe can detect gold buried as deep as $2.5 \mu\text{m}$ below the surface; however, the scanning electron microscope electron beam will reveal only morphological features at the surface; (the electron beam of the scanning electron microscope penetrates to a depth of $\sim 5 \times 10^{-3} \mu\text{m}$). Also, the relatively hard Au X-rays (2,163 keV) resulting from the electron beam bombardment in the microprobe can emerge through thin layers of overlying clay. Figure 11a is another scanning electron micrograph of gold, in this case associated with the organic matter; the gold particles appear as light images. These particles do not show obvious crystalline morphologies. Rather they are thin, flaky-to-filamentous-

►
FIGURE 11 Scanning electron microscope and electron microprobe images of sample VVR-31C from the Vaal Reef carbon seams. (a) Scanning electron photomicrograph of gold particles (light images) associated with organic matter (dark area) in sample VVR-31C from the Vaal Reef. (b) Electron microprobe image of gold associated with clay (3.5x photographic magnification of the area indicated by the arrow in Figure 10d). Note the apparent rectangular, crystalline structure with sharp edges. (c) Scanning electron photomicrograph of the area covering the underlying crystalline gold particles shown by the arrow in Figure 10d (and 11b). The absence of rectangular structures in the scanning electron microscope image indicates that the rectangular gold particles lie buried below the surface; the electron microprobe electron beam penetrates $\sim 2.5 \mu\text{m}$ into the sample and the scanning electron microscope electron beam $\sim 5 \times 10^{-3} \mu\text{m}$. The horizontal dark lines represent in (a) 4 μm , (b) 20 μm , and (c) 10 μm .

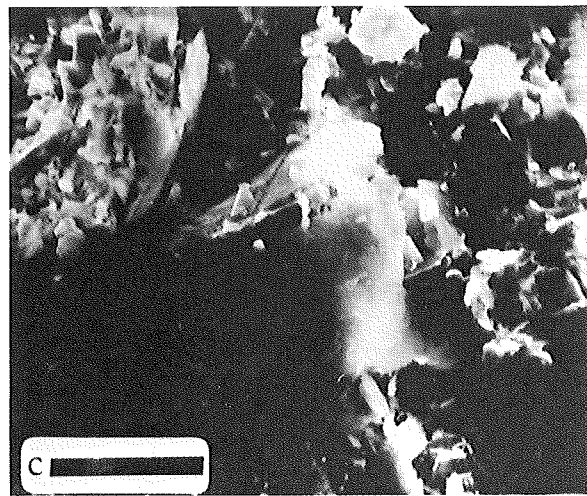
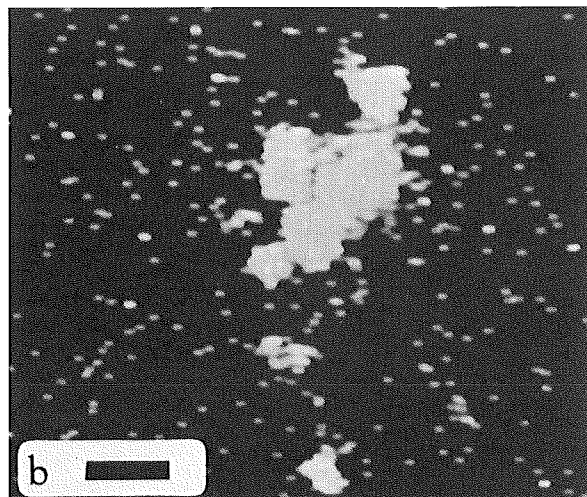
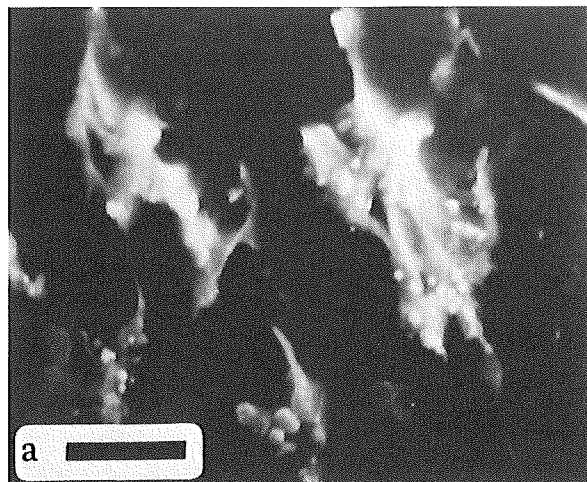


at various magnifications, with the electron microprobe for the following elements: Si, Al, Mg, Fe, S, C, and N. Some of the resulting photographs of the elemental distributions are shown in Figures 10, 11, and 12. Light areas represent enrichment in the specified element.

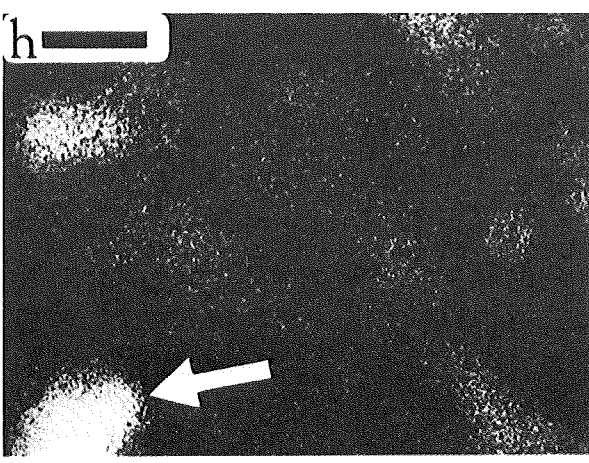
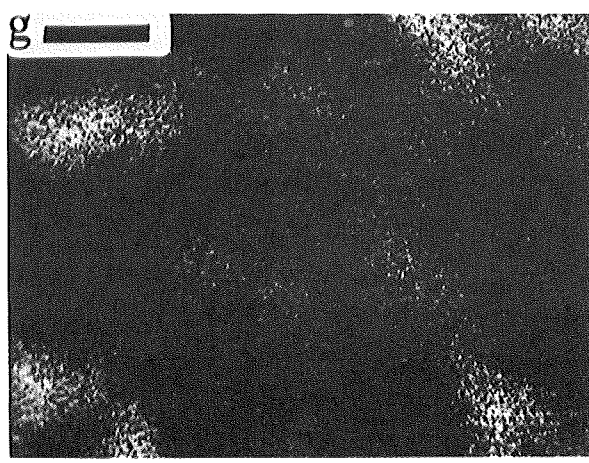
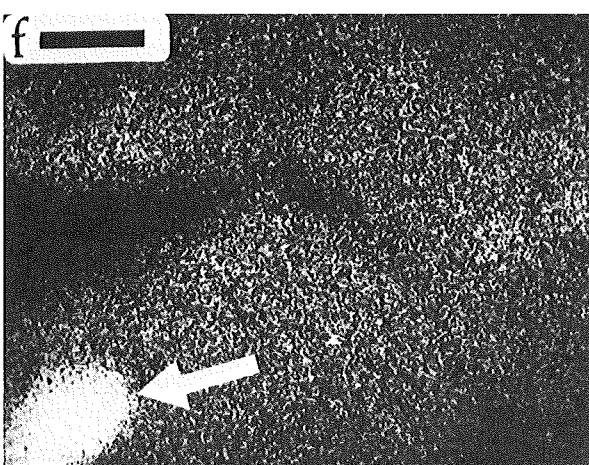
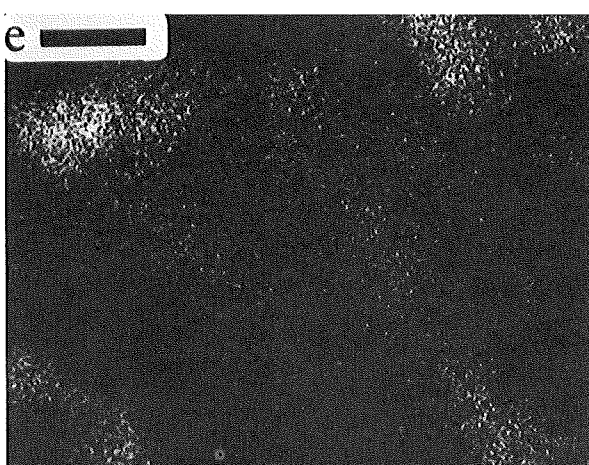
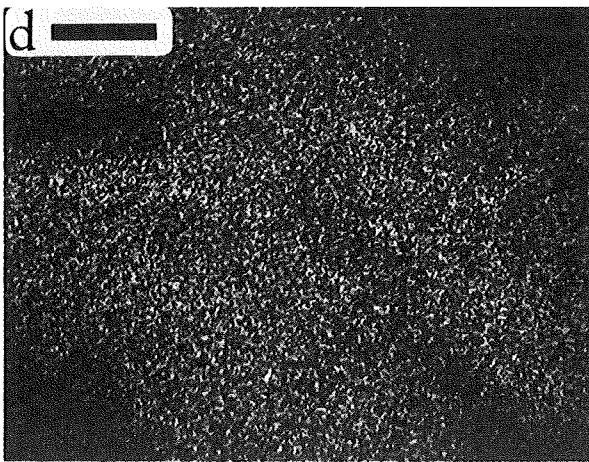
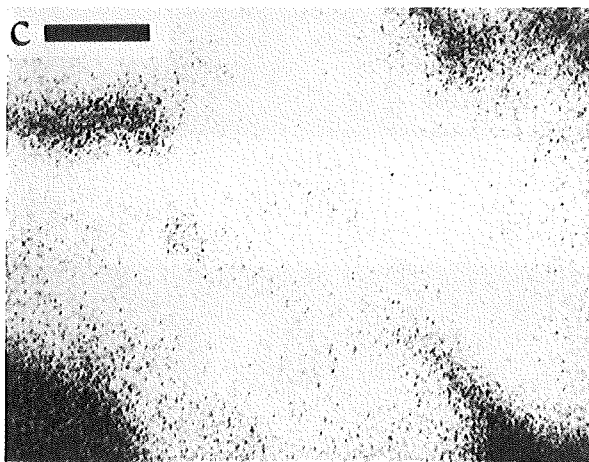
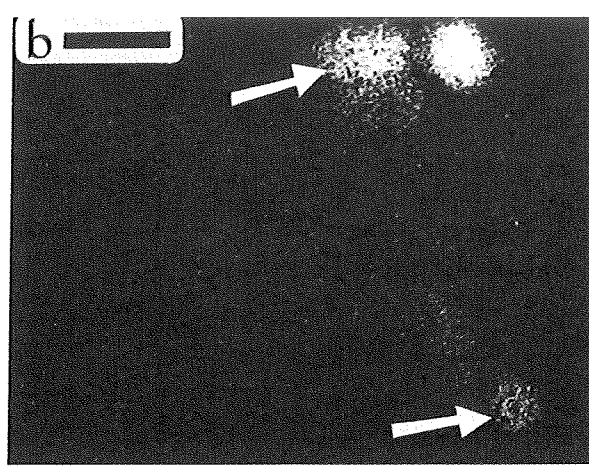
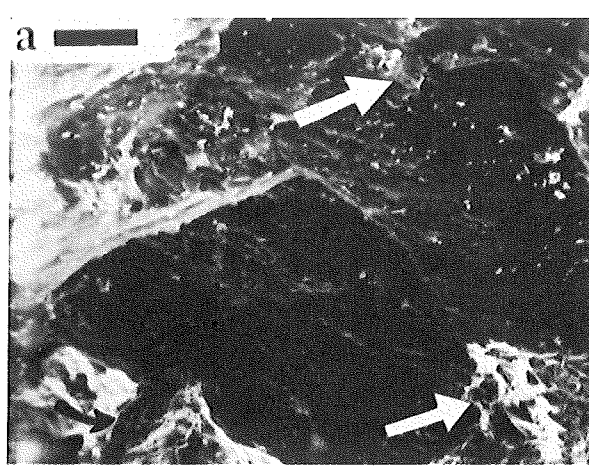
The results of the electron microprobe analyses showed that the carbon seams consisted of two finely admixed substances of different chemical compositions. One of the components contained mainly Si, Al, and Fe together with subordinate amounts of sulphur and gold; S was associated with Fe. Scanning electron micrographs of this component showed the presence of flaky minerals (Figure 11c). Clay minerals were confirmed to be the major components of this substance by X-ray diffraction analyses. X-ray diffraction indicated that the prominent 7.05 Å basal reflexion was probably caused by a sepiitechlorite clay mineral. The other component detected by electron microprobe analyses consisted basically of an organic substance (i.e., the kerogen) containing (non-pyrite) sulphur and occasionally nitrogen in addition to carbon. No magnesium was detected in either of the components that were examined.

Gold frequently occurred adjacent to clay-kerogen boundaries in both the clay and organic phases. A gold particle associated with clay is shown by the arrow in Figure 10d, and photographically enlarged in Figure 11b. The apparent rectangular shape (which can be either an octahedron with its 001 crystallographic axis aligned with the electron beam, or a cube) of this grain of gold is likely the result of the (re)crystallization of dissolved/colloidal gold. However, the great majority of gold particles showed detrital morphology.

The corresponding scanning electron micrograph, Figure 11c, does not show any rectangular minerals; it shows flaky, clay particles. The rectangular gold structures are apparently buried below the surface of the sample. The electron beam of the microprobe can detect gold buried as deep as $2.5 \mu\text{m}$ below the surface; however, the scanning electron microscope electron beam will reveal only morphological features at the surface; (the electron beam of the scanning electron microscope penetrates to a depth of $\sim 5 \times 10^{-3} \mu\text{m}$). Also, the relatively hard Au X-rays (2,163 keV) resulting from the electron beam bombardment in the microprobe can emerge through thin layers of overlying clay. Figure 11a is another scanning electron micrograph of gold, in this case associated with the organic matter; the gold particles appear as light images. These particles do not show obvious crystalline morphologies. Rather they are thin, flaky-to-filamentous-



►
FIGURE 11 Scanning electron microscope and electron microprobe images of sample VVR-31C from the Vaal Reef carbon seams. (a) Scanning electron photomicrograph of gold particles (light images) associated with organic matter (dark area) in sample VVR-31C from the Vaal Reef. (b) Electron microprobe image of gold associated with clay (3.5x photographic magnification of the area indicated by the arrow in Figure 10d). Note the apparent rectangular, crystalline structure with sharp edges. (c) Scanning electron photomicrograph of the area covering the underlying crystalline gold particles shown by the arrow in Figure 10d (and 11b). The absence of rectangular structures in the scanning electron microscope image indicates that the rectangular gold particles lie buried below the surface; the electron microprobe electron beam penetrates $\sim 2.5 \mu\text{m}$ into the sample and the scanning electron microscope electron beam $\sim 5 \times 10^{-3} \mu\text{m}$. The horizontal dark lines represent in (a) 4 μm , (b) 20 μm , and (c) 10 μm .



shaped particles. Figure 12a shows a scanning electron micrograph of the kerogen perpendicular to the bedding plane. The white arrows indicate gold particles, and the black arrow shows a pyrite grain; both Au and FeS₂ were determined by electron microprobe analyses (Figures 12b, f, and h).

Instrumental neutron activation analyses

Major and trace element abundances were determined separately in the kerogen and host rock by instrumental neutron activation analysis (INAA) using the parameters described by Gordon *et al.*²⁴ and Schmitt *et al.*²⁵. Briefly, the technique consisted of bombarding the samples with neutrons in The University of Arizona's TRIGA reactor, which has an average neutron flux of 1×10^{12} neutron cm⁻² sec⁻¹. Nuclei that have been activated by neutron capture in the reactor emit gamma radiation at discrete energies that are characteristic of particular isotopes and by which the elements may be identified. The abundances of gamma rays emitted is indicative of the quantity of a given element in a sample. The activity produced during the irradiation was counted on a 55 cm³ (9.6 per cent efficiency) lithium-drifted germanium detector connected to a Northern Scientific 4096-channel pulse height analyser. Each sample was irradiated twice (5 minutes and 4 hours) and counted at several different times to optimize determinations of radioactive elements with various half-lives. Aliquots of four samples were also re-analysed for uranium using the delayed neutron method of Hamilton²⁶. The values from the delayed neutron method agreed well with the values by standard INAA and gamma radiation counting techniques. The Vaal Reef samples were analysed by comparison with the specific activities produced in synthetic standards activated at the same time under identical conditions. U.S. Geological Survey rock standard GSP-1 also was analysed simultaneously with all samples and the analytical results compared with literature values as a control on the procedure.

The results of the neutron activation analysis are shown in Table 6. They exhibit a wide range of major and trace element abundances in the samples. The largest differences, however, are between the closely adjacent kerogen and their quartzite host rocks, as demonstrated, for example, by comparison of values for WVR-2Q, WVR-2C, and VVR-35Q, VVR-35C (where the host rock is designated by Q and the kerogen separates by C). In particular, gold, silver, uranium, thorium, vanadium, scandium, caesium, antimony, and the rare-earth elements are present in higher concentrations in the kerogen separates than in the quartzite host rock. Only iron, presumably in the form of pyrite or iron-rich clays, shows a fairly even distribution between the carbon seams and the adjacent rocks. Total rocks (from which the kerogen was not separated) have values generally intermediate to the kerogen and quartzitic host rock separates. This points out the necessity of analysing the kerogen by itself.

► FIGURE 12 Scanning electron microscope and electron microprobe images of sample SVR-259T from the Vaal Reef carbon seams. Scanning electron photomicrograph (a) and corresponding electron microprobe images of a selected area on a freshly broken, unpolished surface perpendicular to the bedding plane of sample SVR-259T from the carbon seam. Light areas represent high concentrations of the following elements: (b) gold, (c) carbon, (d) nitrogen, (e) silicon, (f) sulphur, (g) aluminium, and (h) iron. The horizontal dark lines represent 40 µm.

The gold content of the samples is highly variable ranging from 6 p.p.m. in sample VVR-35Q to 1.27 per cent in sample VVR-6C. Obviously, gold is concentrated in kerogen. A comparison of gold with other elements, particularly silver, uranium, and carbon, shows good correlation only between gold and silver. The inferred silver content of the gold is 3.4 to 11.5 per cent with an average content of 6.1 ± 1.9 (1 σ) per cent. This is somewhat lower than the often quoted literature value of more than 10 per cent^{7,27,28}, but falls within the range reported by Viljoen²⁹ who found 0.3 to 32.1 per cent silver in gold grains using an electron microprobe. Low silver contents in gold particles are attributed to preferential solution or leaching of silver during transport of detrital grains^{7,27,28}.

In general, neutron activation analysis proved to be a useful technique in these studies. The presence of large concentrations of uranium, however, resulted in photo-peak interferences in the uranium spectrum at 95 keV (¹⁶⁵Dy), 103 keV (¹⁵³Sm), and at 108 keV (¹⁷⁷Lu) along with uranium fission products. The major fission products produced are zirconium, molybdenum, and two of the rare-earth elements, cerium and neodymium. Although mathematical corrections were applied to the analytical data obtained for these elements, none of them seemed satisfactory and the abundances of these elements have been omitted from Table 6. Zirconium was analysed qualitatively using X-ray fluorescence spectroscopy, which confirmed the presence of this element as a major constituent in the Vaal Reef kerogen. The spectra for titanium and chlorine were not detected in the appropriate short irradiation (1 minute) of samples WVR-2C, WVR-2Q, and VVR-35C, VVR-35Q, indicating that, if present, these elements are in low abundance. The low titanium along with high uranium content would suggest that uranium, in these four samples, is primarily in the form of uraninite (UO_2) rather than brannerite.

As mentioned above, an attempt was made to find correlations between gold and carbon, gold and uranium, carbon and uranium, and some of the other elements determined. Correlation diagrams of these element pairs indicate that the relations are essentially random. The lack of correlation between the total carbon content and gold or uranium agrees with the work of Minter^{30,31}. The correlation of gold and uranium with carbon showed that high concentrations of gold and uranium are associated with high concentrations of carbon; however, high concentrations of carbon often are not associated with the high gold and uranium concentrations. Vanadium concentrations showed close correspondence with those of uranium. However, since only four samples (WVR-2C, WVR-2Q, and VVR-35C, VVR-35Q) were analysed for vanadium this inference should be used with caution.

DISCUSSION

Chemical matrix of the Vaal Reef kerogen

The pyrolysis results indicate that the benzene-methanol insoluble organic matter in the Vaal Reef samples contains condensed aromatic hydrocarbon and aromatic sulphur constituents. These condensed units appear to be connected to each other by short-chain aliphatic hydrocarbon and organic sulphur compound bridges. The condensed aromatic centres are relatively stable because they are not fragmented until 450 °C in high vacuum (10^{-6} torr). The exterior portions of these polymeric units apparently contain some loosely attached/bonded aliphatic components.

TABLE 6
NEUTRON ACTIVATION ANALYSIS OF VAAL REEF SAMPLES:MAJOR, MINOR AND TRACE ELEMENT ABUNDANCES

	C*	U	Th	As	Fe	Na	K	Au	Ag	Cs	Sb
Samples	Values in percent (%)						Values in parts per million (p.p.m.)				
VVR											
35Q	0,03	0,09	0,013	0,033	1,75	0,12	0,70	6	—	4,8	5,2
35C	23,94	3,38	0,386	0,297	6,43	0,05	—	871	71	6,2	51,8
6C	21,07	9,58	1,176	0,172	3,43	0,05	—	12734	758	—	644
8C	13,5	3,79	0,447	0,143	1,70	0,07	0,66	2641	108	3,9	125
21C	17,27	7,52	0,899	0,239	6,97	0,04	—	9217	606	3,1	215
29T	5,46	4,71	0,514	0,091	4,11	0,03	—	7218	446	3,1	262
31C	30,40	1,51	0,137	0,247	0,86	3,27	—	3205	267	479	40,7
SVR											
9T	1,45	0,52	0,054	0,095	2,25	0,07	—	135	—	6,5	14,5
15C	32,35	8,46	1,102	0,604	2,32	0,14	—	5663	518	18,3	310
202C	20,88	9,89	1,170	0,693	10,0	0,08	—	1989	125	—	298
259T	6,15	1,57	0,201	0,169	11,4	0,08	—	1711	97	12,1	51,7
260C	33,73	2,00	0,212	0,093	2,59	0,05	0,48	853	111	—	35,8
WVR											
2Q	0,02	0,29	0,043	0,134	4,12	0,07	0,79	47	—	4,9	10,1
2C	17,98	7,99	0,931	0,225	4,03	0,10	1,10	5440	258	18,0	230
5T	6,14	3,55	0,367	0,637	4,62	0,09	—	1904	66,4	12,3	121
10C	26,14	8,30	1,161	0,571	5,71	0,09	—	5014	263	15,0	149
30C	22,0	1,97	0,307	0,209	9,38	0,04	—	1772	80	4,2	50,8
32C	19,94	9,21	1,210	0,726	8,80	0,08	—	6049	443	—	97,6
35T	0,17	0,11	0,010	0,023	0,38	0,34	2,96	11	—	9,8	3,2
45C	23,2	5,30	1,421	1,295	5,41	0,10	—	4463	189	24,1	304
BVR											
33Q	0,24	1,10	0,097	0,071	9,56	0,04	0,30	513	33,9	4,6	34,6
33C	16,29	5,69	0,668	0,170	8,54	0,04	—	6738	409	5,4	224
46C	7,48	2,66	0,374	1,348	9,95	0,11	1,76	8262	653	7,2	80,2

C: kerogen physically separated from quartzite
Q: adjacent quartzite physically separated from kerogen
T: whole rock

n.d.: not determined
—: below detection limits

* : determined by conventional oxidative combustion analyses by Schwartzkopf Microanalytical Laboratory, Woodside, N.Y.

TABLE 6
NEUTRON ACTIVATION ANALYSIS OF VAAL REEF SAMPLES:MAJOR, MINOR AND TRACE ELEMENT ABUNDANCES (cont'd)

	Co	Hf	Sc	La	Eu	Tb	Yb	Ta	Mn	V	
Samples	Values in parts per million (p.p.m.)										
VVR											
35Q	69	10	4,6	64	2,35	1,3	3,8	3,4	107	—	210
35C	415	136	32,2	243	20,4	22,2	79,6	21,9	542	n.d.	n.d.
6C	342	291	50,4	584	81,3	96,3	642	172	n.d.	n.d.	n.d.
8C	226	144	21,6	275	33,5	27,8	172	7,4	n.d.	n.d.	n.d.
21C	339	231	28,7	321	34,1	34,8	156	43,1	n.d.	n.d.	n.d.
29T	242	166	16,9	330	49,2	23,6	151	8,0	n.d.	n.d.	n.d.
31C	260	74	6,8	64	25,8	13,3	68	31,5	n.d.	n.d.	n.d.
SVR											
9T	144	19	6,3	61	6,16	5,1	26,1	4,5	n.d.	n.d.	n.d.
15C	877	245	82,2	475	56,9	28,5	242	37,2	n.d.	n.d.	n.d.
202C	717	364	95,4	430	99,9	127	536	72,3	n.d.	n.d.	n.d.
259T	406	74	24,4	273	22,3	7,5	28,4	15,7	n.d.	n.d.	n.d.
260C	131	66	13,0	103	16,6	22,2	71,9	18,5	n.d.	n.d.	n.d.
WVR											
2Q	237	40	9,0	118	3,87	3,6	11,0	2,9	153	39	
2C	303	270	43,6	523	38,4	58,6	289	14,3	1023	912	
5T	823	122	28,9	284	14,6	14,5	103	10,2	n.d.	n.d.	
10C	754	390	73,9	587	58,7	39,7	193	51,9	n.d.	n.d.	
30C	526	143	73,5	198	36,6	17,7	121	29,2	n.d.	n.d.	
32C	941	361	87,1	499	62,7	52,2	252	28,7	n.d.	n.d.	
35T	51	5	12,9	68	2,74	1,3	7,7	6,6	n.d.	n.d.	
45C	1323	382	51,9	593	51,7	62,2	437	103	n.d.	n.d.	
BVR											
33Q	263	31	15,3	105	11,86	8,8	42,7	16,7	n.d.	n.d.	
33C	370	143	34,3	334	49,5	31,6	143	43,0	n.d.	n.d.	
46C	2057	87	32,7	212	16,5	19,5	92,8	58,0	n.d.	n.d.	

C: kerogen physically separated from quartzite
Q: adjacent quartzite physically separated from kerogen
T: whole rock

n.d.: not determined
—: below detection limits

The possibility that the organic sulphur compounds were synthesized from pyrite and aromatic hydrocarbons by secondary reactions during pyrolysis is remote. Classical elemental analyses and microprobe determinations show that non-pyrite sulphur is present in the kerogen. Also, the quantity of sulphur compounds in the pyrolyzates such as methylthiophene and benzothiophene etc., show no correlation with the relative amounts of pyrite found in the same samples by X-ray diffraction analyses. Elemental sulphur would have been removed by solvent extraction prior to pyrolysis.

A control experiment was also performed to confirm that aromatic sulphur compound artifacts were not formed during pyrolysis. Finely powdered pyrite was mixed with the condensed aromatic hydrocarbon compound perylene, and pyrolyzed at 450°C after degassing at room temperature under 10^{-6} torr vacuum. CO_2 , SO_2 , propene, xylene, and small quantities of COS and CS_2 were identified. No aliphatic or aromatic sulphur compounds were detected among the pyrolysis products. This experiment indicates that only gaseous carbon-sulphur compounds are formed from pyrite and this aromatic hydrocarbon under the conditions used for the Vaal Reef kerogen pyrolysis. The oxygen in some of these pyrolysis products was probably derived from residual atmospheric oxygen or iron oxide impurities in the pyrite. Thus, it appears that aromatic sulphur compounds are indigenous to the Vaal Reef kerogen.

Search for correlations between organic constituents and uranium and gold contents

Different Vaal Reef kerogen samples showed relatively minor variations among the abundances of their pyrolysis products. Quantities (derived from gas chromatographic peak areas) of some of the pyrolysis products were determined in ten different samples containing varying amounts of uranium and gold. Ratios of selected, well-defined peak areas from each chromatogram were compared with the corresponding uranium or gold contents. Ratios of pyrolysis products must be used to normalize the results because the quantities of breakdown products were affected by the different amounts of samples pyrolyzed and by the relative kerogen abundances in the samples. No apparent correlation was found between any of the measured organic compounds and gold. These compounds included *o*-xylene (7), *n*-propylbenzene (8), methylethylbenzene (9),

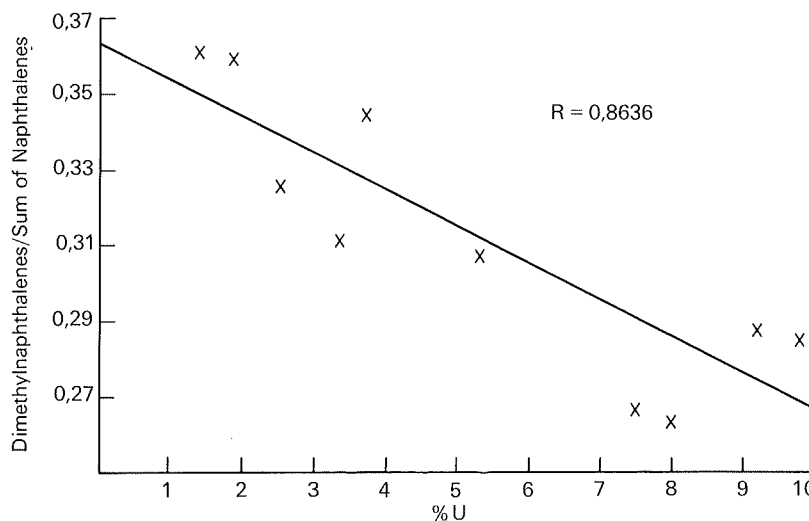
trimethylbenzene (11), methylpropylbenzene (13), naphthalene (20), 2-methylnaphthalene (23), 1-methylnaphthalene (24), ethylnaphthalenes (25, 26), and dimethylnaphthalenes (27, 28, 29), where the numbers in parentheses refer to the gas chromatographic peaks in Figures 2 and 3. However, it was not possible to calculate the > 1000 possible individual and combined abundance ratios of compounds or the > 10000 possible ratios from the ten different samples. Systematic computer searches may yet reveal a correlation between gold and some pyrolysis product ratio(s). One problem encountered in these correlations is the accurate determination of the gas chromatographic peak areas; some of the peaks have shoulders and/or are overlapped by minor components that give ambiguous results. However, many of the compounds measured, especially the alkynaphthalenes, exhibit well-defined peaks and their mass spectra showed only single compounds.

The uranium content and the abundance of the dimethylnaphthalenes showed an inverse correlation. The dimethylnaphthalenes decreased in abundance relative to other alkynaphthalenes as the uranium content increased. This correlation is shown in Figure 13. Since it is more difficult to cleave the aromatic carbon-carbon double bonds than those in the alkyl bridges and because of other physical-chemical considerations, an abundance of dimethylnaphthalenes could represent a somewhat less aromatic matrix than the matrices of kerogens where those components are not as abundant. Consequently, the decrease of dimethylnaphthalenes relative to all other naphthalenes may imply a more aromatic kerogen with increasing uranium content, which is in agreement with the effect of prolonged irradiation from uranium as will be discussed later.

Rare-earth and variable valence elements

The rare-earth elements (lanthanum to lutetium in the Periodic Table) are unique because they tend to behave as a coherent group rather than as a number of individual elements during terrestrial geological processes. They may be fractionated during the crystallization of igneous rocks, e.g., europium may be reduced from the $3+$ state to the $2+$ state depending upon the oxygen content of the magma, and thus can become chemically separated from the rest of the rare-earth elements. However, the rare

FIGURE 13 Correlation between uranium content and the ratio between dimethylnaphthalenes and all naphthalene compounds. R is the coefficient of correlation ($R = 1.0000$ in a perfect correlation).



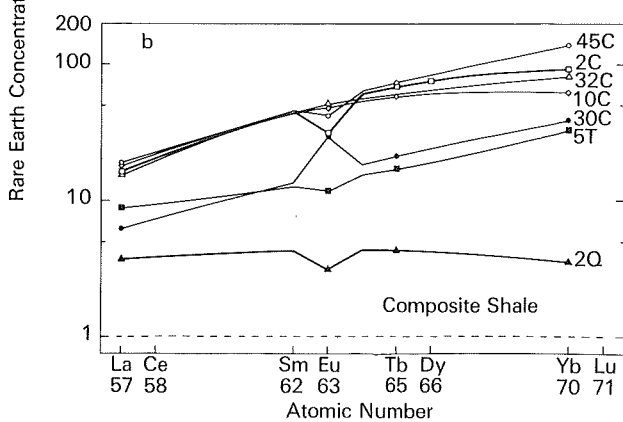
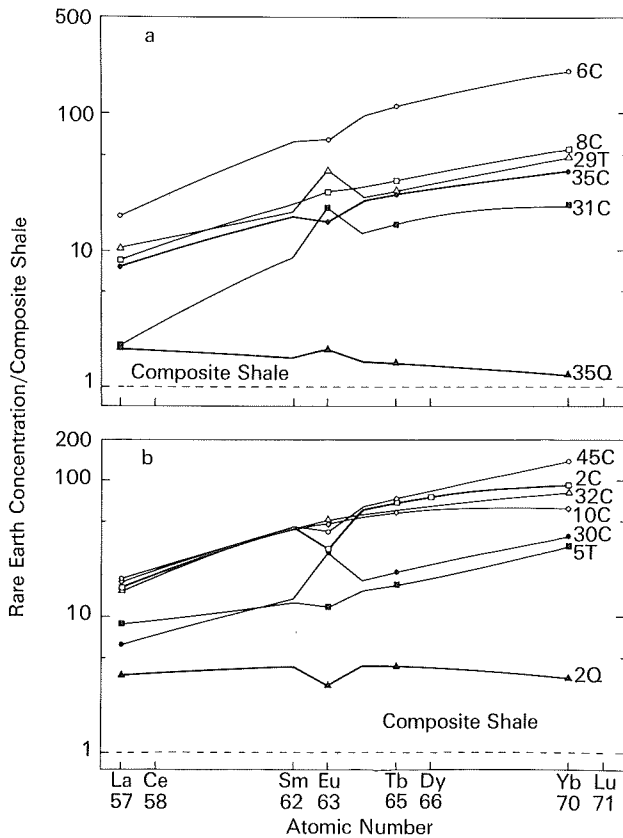
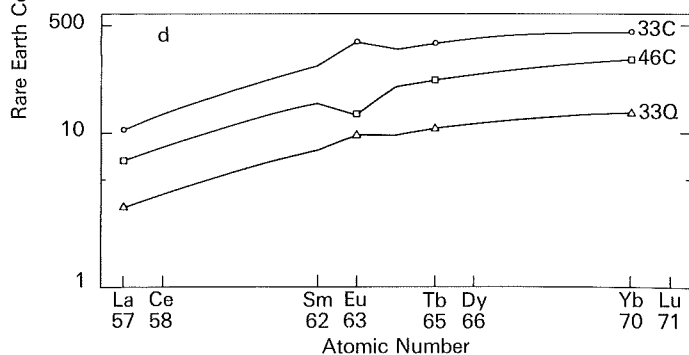
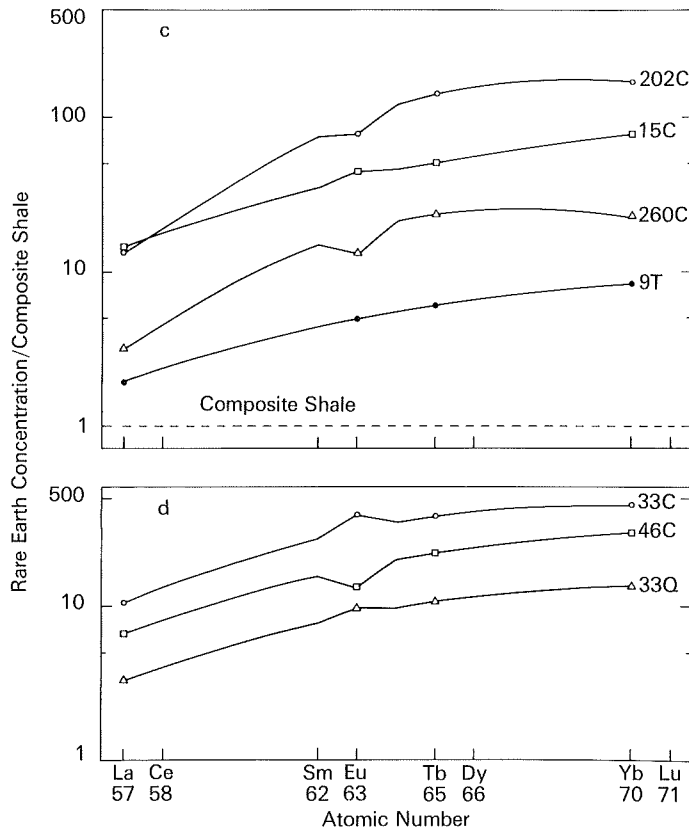


FIGURE 14. Comparison of rare earth element contents in (a) VVR samples, (b) WVR samples, (c) SVR samples, and (d) BVR samples. As in previous designations, the letter C after the sample number defines kerogen separates, Q quartzite host rock separates, and T unseparated total rock samples.

earths are generally re-mixed by weathering and sedimentation into their crustal average relative abundances^{32,33}. Rare earth abundances were treated according to the procedure of Coryell *et al.*³⁴, in which samples are normalized by dividing the concentration of each element by its abundance in a reference material, such as the North American shale composite³⁵. Deviations in abundances from average crustal rocks, as represented by the shale composite, are apparent with this type of sample normalization. The abundances of the rare earth and variable valence elements determined in this study are listed in Table 6.

The Vaal Reef samples analysed contain higher rare earth element abundances by factors of 2 to 100 more than average crustal rocks. Some differences in rare-earth elemental distribution patterns occur among samples from different localities within the Vaal Reef (Figure 14). Rare earth averages obtained from kerogen separates (Table 6) from each mine show that the VVR samples and the WVR samples have La/Yb ratios of 1.33 and 1.86 respectively. The BVR samples, located east of the WVR and VVR areas, have a La/Yb ratio of 2.32. Their distribution pattern shows a slope less than those of the VVR and WVR samples as is illustrated in Figure 15. The SVR samples have a La/Yb ratio of 1.19. Sample VVR-21C has a rare-earth pattern similar to the SVR samples, suggesting some geological relation between the two sample areas. Generally, the variations in rare-earth distribution patterns may indicate differences in the absolute abundances of certain minerals.

Within specific suites of samples the kerogen separates are enriched in rare-earth elements relative to the quartzite host rocks. In the pairs WVR-2C, WVR-2Q, and VVR-35C, VVR-35Q, the quartzite (Q) pattern shows a decline



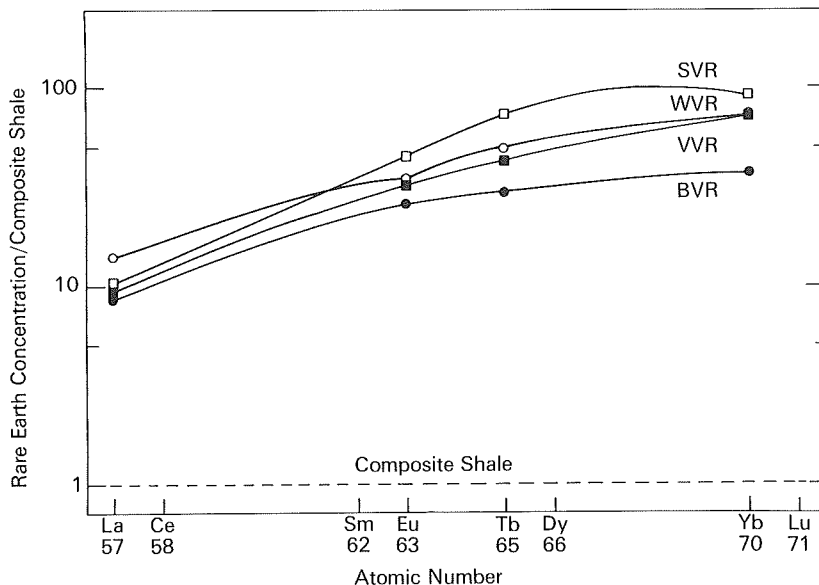


FIGURE 15 Comparison of average earth contents from kerogen separates of VVR, WVR, BVR, and SVR samples.

from lanthanum to ytterbium which represents a reverse trend relative to the corresponding kerogen (C). The respective rare earth curves for the sample pair BVR-33C-BVR-33Q are similar, only the total concentrations differ. These relations are illustrated in Figures 14a-d. A number of samples showed a slight excess or depletion of europium compared to the other rare-earth abundances. Moderate fluctuations of europium content in sedimentary rocks are influenced by the composition of the source rocks from which the sediments were derived^{33,36,37}.

As noted, kerogen samples are disproportionately enriched in the heavy rare-earth elements. The only known mineral that has a heavy rare-earth enrichment of this magnitude is zircon. Rare-earth abundances published in the literature for zircons³⁸ and several other minerals are shown in Figure 16 for comparison. Recent analyses of micas and clay minerals have shown that both of these

phylosilicates contain highly variable quantities of the rare-earths owing to their ability to adsorb these elements on their crystal surfaces during weathering and sedimentation^{36,39}. It should be emphasized that although the rare earth abundance curves for the Vaal Reef samples may be reconstructed by a judicious choice of the proper proportions of the minerals shown in Figure 16, there is little information on rare-earth abundances in pyrite, gold, or uranium-bearing minerals. Analyses on these latter minerals, along with a suite of complete mineral separates from the Vaal Reef samples, could result in more definite relations.

Metamorphism should not have affected the distribution of these elements in the Vaal Reef. There is general agreement that no fractionation occurs among the rare-earth elements during metamorphism⁴⁰. It should be noted in this connexion that the preservation of potential

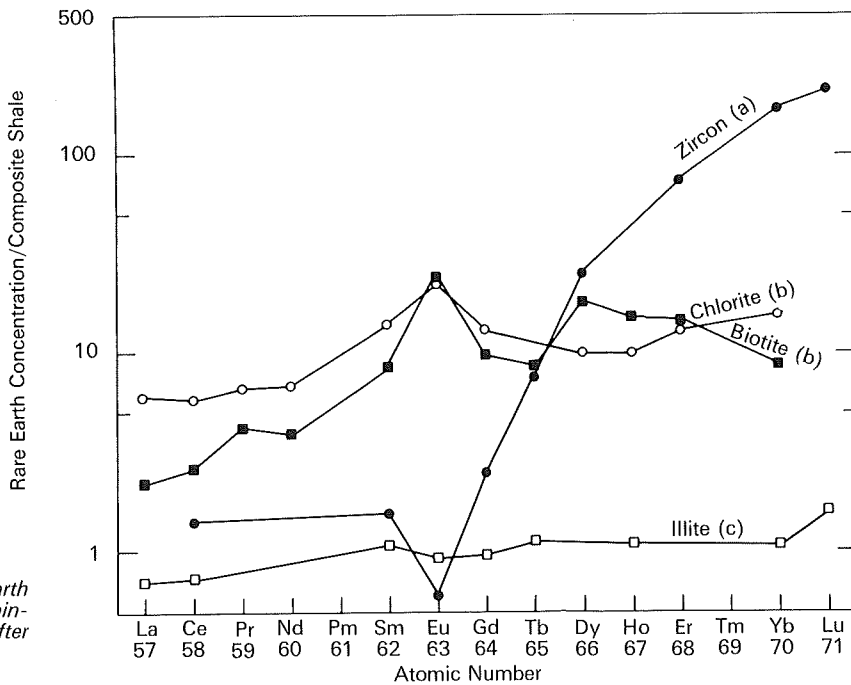


FIGURE 16 Comparison of rare-earth element abundances in relevant minerals: (a) after Nagasawa,³⁸ (b) after Roaldset,³⁶ (c) after Cullers et al.³⁹.

microfossils in the Vaal Reef kerogen^{41,42}, precludes severe temperature history(ies). As was shown, the C/H atomic ratios of kerogen fall mainly within the bituminous coal rank, which also indicates a low metamorphic grade.

Studies of the rare-earth element contents of Precambrian rocks from the North American, Baltic, and African shields suggest that sedimentary rocks have apparently had the same relative rare-earth element abundances during the past $\sim 3 \times 10^9$ years^{33,43}. Therefore, deviations from crustal abundances in the Vaal Reef samples must be caused by preferential concentration of certain minerals, which results in the selective accumulation of the rare-earth elements. In particular, these include zircons, clay minerals, and micas. Quartz contains a relatively low abundance of the rare-earth elements and it acts as a dilutant to total concentrations as may be readily observed from the Vaal Reef quartzitic host rock abundances.

The thorium to uranium ratio in the samples that were analysed averaged 0,12. This value is approximately 30 times lower than the average Th/U ratio of igneous (3,5 to 4) and sedimentary (3 to 4) rocks⁴⁴. Thorium and uranium are typically covariant in igneous rocks. Uranium and thorium may be separated during weathering and sedimentary processes because uranium may be oxidized to the soluble uranyl ion (UO_2^{2+}) and because thorium is relatively insoluble in water. The soluble uranyl ion will precipitate from solutions by reduction to the 4+ valence state in the presence of organic matter^{45,46,47,48}. Since the Th/U ratios in the Vaal Reef samples are significantly below 1, this indicates that substantial fractionation has occurred between thorium and uranium in the Vaal Reef sediments. Since much of the uraninite is in the form of detrital grains^{31,49}, only part of the uranium was dissolved during transport and sedimentation. It has been noted that many of the uraninite particle morphologies in the kerogen may indicate recrystallization⁵⁰. This may have occurred after the precipitation of the uranyl ion in decaying microbial matter which, from modern analogues, is known to contain a reducing environment.

Antimony shows a strong enrichment in the Vaal Reef kerogen samples; abundances as high as 644 p.p.m. have been determined. The average abundance of antimony is 0,2 p.p.m. in igneous rocks and 2,0 to 2,6 p.p.m. in soils and sedimentary rocks. Its concentration in coals varies between 35 to 3 000 p.p.m.⁵¹. Antimony, like uranium, is soluble in the oxidized state (Sb^{5+}) and tends to precipitate in the reduced state (Sb^{3+}). This is in agreement with the uranium-thorium fractionation process.

Chemical history of the Vaal Reef kerogen

According to the current concept the source of the Vaal Reef kerogen was primitive micro-organisms consisting in part of blue-green algae^{7,30,42,52}. The major biochemical components of blue-green algae are: 35 to 73 per cent proteins, 12 to 66 per cent carbohydrates, and 4 to 9 per cent lipids on a dry weight basis⁵³. These fundamental biochemicals also occur in high abundances in other primitive micro-organisms. Two questions arise in this connexion. First, what processes converted the microbial biochemicals into the random aromatic polymer of the Vaal Reef kerogen? Second, how can one account for the relative absence of the organic oxygen and nitrogen compounds in the kerogen which are so abundant in the biochemicals?

It needs to be emphasized at the beginning of this discussion that biochemicals in micro-organisms contain few

aromatic compounds. Some of the amino acids that make up proteins, such as phenylalanine, contain aromatic units. However, such compounds occur in far less quantities than would be sufficient to account for the overwhelming aromatic nature of the Vaal Reef kerogen. In this connexion, one may consider that coals also are generally aromatic substances; however, their origin can usually be traced to higher plants that did not evolve until the Paleozoic and that contain an abundance of lignin, a high aromatic biopolymer. Most coals were formed from sources that contained initially large quantities of lignin. This was not the case with kerogens formed from microbial sources. Still, most typical Precambrian kerogens are aromatic in nature and contain organic oxygen and nitrogen compounds. Their aromaticity is usually attributed to thermal maturation and diagenesis during geologically long periods of time.

One of the important properties of the Vaal Reef carbon seams is its high uranium abundances. Several of the kerogen samples analysed by neutron activation contained from one to almost ten per cent uranium by weight. The radiation emitted by this radioactive element over thousands of millions of years could well have been another principal factor that initiated polymerization and contributed to the aromatization of the Vaal Reef kerogen. The radiation emitted through the decay of the natural isotopes of uranium are mainly alpha particles (helium nuclei) with energies between four and five million electron volts, beta particles (high energy electrons), together with gamma radiation. During a period of 2500 million years, uranium (^{238}U and ^{235}U) in the Vaal Reef kerogen produced $\sim 2,2 \times 10^{21}$ alpha and $\sim 1,6 \times 10^{21}$ beta particles per gram of kerogen carbon. When these particles collide or interact with organic compounds they usually produce free radicals.

As was mentioned before, three Vaal Reef samples were analysed by electron paramagnetic resonance spectroscopy. The results of these analyses (Table 5) indicate a large concentration of spins or free radicals per gram of kerogen carbon. This concentration is from ten to one hundred times greater than the organic free radical concentrations normally found in coals. Concentrations in the coal macerals vitrinite and fusinite (which are petrographic components of coal) vary between 5 to 20×10^{18} spins/gram carbon and 30 to 60×10^{18} spins/gram carbon, respectively⁵⁴. The Vaal Reef samples contained $\sim 4 \times 10^{20}$ spins/gram of kerogen carbon. The quantity of alpha and beta particles produced during a period of ~ 2500 million years is compatible with such an abundance of free radicals. Also, the electron paramagnetic resonance spectral curve widths of the high rank coal maceral vitrinite is 4,5 to 7,0 gauss, and the width of the lower rank coal maceral, fusinite, is 2 to 3 gauss⁵⁴. The spectral curve widths of the Vaal Reef samples, 2,8 to 4,1 gauss, generally correspond to those of the fusinite coal component. This is interesting because fusinite is neither the most aromatic component of coals nor the one indicating effective diaxygenic and metamorphic alterations.

Normally, free radicals are unstable and are highly reactive entities. However, they can be stabilized if the unpaired electrons are distributed throughout an extensive organic matrix containing alternating double bonds⁵⁵, such as in the aromatic matrices of coal, petroleum asphaltenes (i.e., the solid organic matter in crude oil), and the Vaal Reef kerogen, etc. Because these substances are

solids, the motion of their molecular components are virtually restricted in the matrices; this hinders free radical reactions.

Stable organic free radicals can be formed by different processes in kerogen and its precursors. Some of the free radicals form early in the organic matter in sediments. For example, a significant concentration of free radicals ($\sim 10^{17}$ spins/gram carbon) can already be present in modern humic substances⁵⁵, which consist of recently decayed biological matter and their reaction products. Breaking of bonds (which is also called bond scission) by the effect of heat during diagenesis and the concurrent release of various volatile components may also give rise to the formation of free radicals in coals and kerogens. However, the excess of free radicals in the Vaal Reef kerogen must be attributed, in all probability, to irradiation from uranium. It has been reported⁵⁶ that in 20 million years $\sim 10^{16}$ spins/gram carbon will be produced in organic substances similar to kerogen which contain only 1 p.p.m. uranium. By simple extrapolation, kerogens containing 10 000 p.p.m. (1 per cent) uranium would contain $\sim 10^{22}$ spins/gram of carbon after 2000 million years of irradiation. This value is higher than those of the free radical concentrations found in the Vaal Reef kerogens. The discrepancy may be reconciled if there is a saturation, or equilibrium, point in the Vaal Reef aromatic organic polymer, i.e., a state where as many free radicals recombine as are newly formed by irradiation. As the density of free radicals increases in the kerogen matrix, it seems likely that the chances of recombination also increase and a saturation point may be reached.

The chemistry of organic free radicals and the effect of irradiation on common biochemicals and biopolymers needs to be reviewed before attempting to explain the various possible mechanisms which produced the Vaal Reef kerogen from its microbiological precursors. A recent review of the chemistry of free radicals is given by Huang *et al*⁵⁷. There are two major types of free radical reactions. The first involves free radical combination where two radicals join to give non-radical products. The second reaction consists of free radical transfer. This process generates new free radicals. These two main categories can be subdivided into more specific types of reactions. Combination or coupling of two radicals leads to bond formation and a non-free radical molecule. What is called a disproportionation type reaction involves the transfer of a hydrogen atom from one free radical to another one yielding non-radical products. This type of a reaction often leads to unsaturated products (i.e., loss of hydrogen) and an increase of aromatic components. Certain types of free radicals can act as oxidizing (HO^\cdot) or reducing (aromatic radicals) agents when they are combined with transition metal ions. (The dots adjacent to atoms represent unpaired electrons, i.e., the free radicals.) Another mechanism, which is called displacement of radicals, may also occur; this usually involves the removal of hydrogen. Furthermore, the addition of free radicals to double bonds usually gives a more stable radical and often leads to polymerization. During what is called fragmentation, a radical breaks down by bond scission to give a smaller radical and an unsaturated molecule. Another free radical reaction, which is called radical aromatic substitution, takes place when a hydrogen atom is relocated on an aromatic molecule. This reaction can form polycyclic aromatic compounds, i.e., structures in which several

aromatic rings are fused together. These examples illustrate the diversity of organic chemical reactions caused by free radicals.

Many polymerization reactions are carried out in the laboratory and industry by some of the free radical mechanisms described above. An initiator agent (such as irradiation) is needed first to form an initial small radical that can then affect free radical transfer to the unit components of the polymer, i.e., to the monomers. The polymerization reaction is propagated when the monomer radical combines with another monomer molecule to give a larger free radical. This process is repeated and the polymer grows larger until termination reactions occur, such as the recombination of two radicals; if enough recombination reactions occur the polymerization process ceases. Also, when molecular movement is restricted and monomer molecules are depleted, the polymerization process can be terminated, even though free radicals may still remain. The monomeric molecules do not have to be identical, and in the case of coal, other natural organic substances, and the Vaal Reef kerogen, there must have been a great variety of monomeric organic radicals which polymerized in a random sequence.

Next, it seems appropriate to review briefly the effects of irradiation on organic and biochemical compounds. Generally, when biochemicals, such as proteins, carbohydrates, lipids, etc., are irradiated, they are fragmented and/or become connected by bridges (crosslinking). This is usually accompanied by the loss of hydrogen and it often leads to double bond formation⁵⁸. The fragmentation products are generally small molecules such as CO , CO_2 , H_2 , NH_3 , etc. Scission leads to breaking of bonds and a decrease in molecular weight; crosslinking leads to an increase in molecular weight and the formation of a network type matrix. These reactions apparently proceed via free radical intermediates. This can be accomplished either directly or indirectly, i.e., the radiation either affects the organic molecule directly producing a free radical, or the solvent that contains organic molecules is itself affected and forms free radicals. Subsequently, these radicals produced from the solvent undergo radical transfer or redox reactions, as was outlined above, with the dissolved/dispersed organic molecules. The ubiquitous solvent in biological systems is water. Irradiation of water yields several reactive free radicals and ionic species. A schematic reaction of the radiolysis of water can be expressed as: $4\text{H}_2\text{O} \rightarrow \text{O}_2 + 3\text{H}_2 + \text{H}_2\text{O}_2$ ⁵⁹. The major intermediate free radicals that play a role in this reaction are HO^\cdot and H^\cdot ; they react with each other, with neutral molecules (H_2O , O_2 , and H_2O_2), and with ionic species (e.g., OH^- , H^+ , H_3O^+ , etc.) in a variety of ways to give O_2 , H_2 , and H_2O_2 as well as newly formed water as the end products. The intermediate free radicals produced from water can also react with organic matter producing organic radicals that then can undergo reduction or oxidation, polymerization, fragmentation, etc.

It has long been known that amino acids undergo deamination, that is the release of free ammonia, upon irradiation^{58,59,60,61,62,63}. For example, the amino acid, glycine, yields ammonia and formaldehyde while another amino acid, alanine, gives ammonia and acetaldehyde⁶⁰. Both H_2S and sulphide bonds are often produced when the sulphur-containing amino acids are irradiated. These reactions are believed to occur through an indirect pathway where free radicals arising from irradiated water

(H⁺ and HO⁻) attack the amino acid molecule. Bonds connecting amino acids in the protein biopolymer are broken during irradiation⁵⁹. Like their components, the amino acids, proteins also liberate ammonia and hydrogen sulphide when irradiated. It is interesting that the irradiation of meat, which is rich in protein, yields alkylbenzenes, alkyl sulphides, and acetaldehyde⁵⁸. The irradiation of proteins yields products that are similar to those found in the Vaal Reef kerogen. One must hastily add that this reference by no means implies that animal life evolved by Witwatersrand time. However, as is well known, primitive micro-organisms also contain proteins.

Irradiation of sugars with gamma rays results in electron paramagnetic resonance spectra showing the generation of free radicals⁶⁴. Generally, polysaccharides, e.g. starches, are broken down to their individual sugar constituents upon irradiation^{58,59,60}. Another polysaccharide, cellulose, is randomly ruptured along its polymeric chain and yields its corresponding sugar (glucose) component⁶⁰. It appears that the irradiation of simple sugars, such as glucose, results in the production of the corresponding uronic acid, e.g. glucuronic acid^{58,65}. The amount of acid produced is independent of the sugar concentration which implies indirect action by free radical intermediates from water. Formaldehyde is also produced which implies carbon-carbon bond cleavage^{60,66} and the destruction of the individual sugar units. Irradiation of DNA (deoxyribonucleic acid), a genetic biopolymer, results in polymer fragmentation into intermediates, which subsequently release ammonia^{58,59,60}. Chlorophyll can also be partially destroyed by irradiation⁶⁰.

Irradiation of saturated hydrocarbons (i.e., those which contain no double bonds) liberates predominantly hydrogen with lesser amounts of methane, etc.^{58,60}. The effect of irradiation on non-aromatic hydrocarbons containing double bonds (olefins) often leads to high molecular weight crosslinked polymers⁶⁰. Aromatic hydrocarbons are more stable upon irradiation than the saturated hydrocarbons^{60,67}. Other organic compounds such as alcohols produce hydrogen, methane, carbon monoxide, and saturated and unsaturated hydrocarbons upon irradiation⁶⁰. Ethers often react to form alcohols and olefins, while certain products of fatty acids, such as their esters, lose H₂, CO₂, and CO and may lead to the production of crosslinked polymers⁶⁰. Organic acids often lose CO₂ and H₂ during irradiation and yield unsaturated hydrocarbons together with polymerized products^{60,68}. This brief review shows that free radical and radiolysis reactions are complex processes. When thermal and other diagenetic factors are also considered, it becomes apparent that the evolution of the Vaal Reef carbon seams was a complicated chemical procedure.

CONCLUSIONS

Currently available evidence and observations strongly suggest that the precursors of the Vaal Reef carbon seams were primitive microbial mats. In modern analogues layers of living micro-organisms are continuously superimposed on dead and/or decayed microbial matter in the mat. In such an ecosystem, a variety of biochemicals are present in the living micro-organisms; these substances are released upon the death of the microbiota and subsequently the biochemicals react with one another. Generally, parts of the mats have a network-like texture

consisting of filamentous micro-organisms or their resistant remnants. Detrital particles, including uranium minerals and gold, may be trapped and held in the mat matrices.

Major and trace element abundances in the Vaal Reef kerogen generally support a detrital origin for most of the gold and uranium as is shown by the silver content of the gold and the rare-earth element abundance patterns. However, the thorium-to-uranium ratios indicate that part of the uranium was oxidized to the soluble uranyl ion prior to the final emplacement in the mats. Subsequently, uranium precipitated out under the reducing environments known to exist in decayed microbial mats. Also, the high antimony abundances suggest a similar oxidation-reduction history and concentration.

Some of the gold particles in the Vaal Reef carbon seams show grain morphologies that are not compatible with a detrital origin. Fatty and amino acids are common constituents of primitive micro-organisms; these major biochemicals contain carboxyl groups. The carboxyl groups of these organic compounds and the uronic acids, which are derived from the degradation of sugars, could have stabilized colloidal gold and/or gold organic polymeric substances during low temperature transport by water. A similar mechanism has been proposed already for stabilizing colloidal gold during transport⁶⁹. Such mechanisms could have been effective during low-energy transport of gold from its primary source to the microbial mats. The organic substances needed for the stabilization of gold could have been derived from micro-organisms growing in hot pools near the gold source area and in water around river banks. After such gold-organic complexes reached and became incorporated in the microbial mats, gold could have crystallized out *in situ*.

After the uranium minerals became incorporated in the microbial mats, in all probability many of the mat biochemicals broke down into smaller molecules because of the irradiation emitted by uranium. Irradiation of water is expected to have played a role in this process. From what is known about the irradiation of proteins and amino acids, it appears that these substances in the original Vaal Reef mats must have lost much of their nitrogen content, and released ammonia. This could explain the failure of detecting volatile nitrogen containing organic compounds in the Vaal Reef samples during analysis by pyrolysis. It is interesting in this connexion that other Precambrian kerogens from southern Africa etc. of comparable age and biological origin, e.g. the Transvaal and Bulawayan stromatolites, yielded various organic nitrogen compounds upon pyrolysis⁶. These rocks, however, lack appropriate concentrations of uranium.

During diagenesis of the Vaal Reef sediments, organic free radicals (molecules with unpaired electrons) were formed because of radiation emitted by uranium, heat during diagenesis, etc. The decayed substances began to polymerize, losing volatiles such as H₂, CH₄, CO₂, and NH₃. Free radical fragmentation reactions were probably responsible for the formation of unsaturated molecules, that is compounds containing double bonds. This contributed to the initial step in the polymerization and aromatization process. The fragmentation and many polymerization reactions are endothermic and are favoured by an increase in temperature⁵⁷. Reactions known in polymer chemistry, such as free radical polymerization, disproportionation, displacement, and addition reactions, probably

all contributed to the formation of the Vaal Reef polymer. Free radical aromatic substitution mechanisms may have been responsible for the end stages of the development of the aromatic Vaal Reef kerogen. The organic substances which consist of several fused aromatic rings connected by saturated hydrocarbon chain bridges can be formed by this process. The aromatic hydrocarbons are more stable to irradiation than the saturated hydrocarbons and this increase of stability appears to be one of the causes for the highly aromatic nature of the Vaal Reef kerogen.

The Vaal Reef kerogen is an insoluble random aromatic polymer which contains an unusually high concentration of organic free radicals. Because of continuous decay of uranium isotopes, free radical formation has persisted throughout the entire history of the Vaal Reef organic matter. The amount of energy from alpha and beta particles to which one gram of Vaal Reef kerogen carbon was subjected during a period of ~ 2500 million years is more than one half of one million kilocalories or more precisely, 1.6×10^{22} million electron volts.

Thus, the Vaal Reef carbon seams developed from primitive micro-organisms and concentrated gold and uranium through a variety of complex organic chemical and physical processes. Uranium has influenced the evolution of the Vaal Reef carbonaceous matter by affecting the alteration of biochemicals from the progenitor, microbial sources to the insoluble and random aromatic polymer. As was noted above, the radiation effect was one of the major factors, but certainly not the only factor that affected the evolution of the kerogen. Since modern organic geochemical methods are capable for elucidating the evolution of organic-ore mineral associations, organic geochemistry emerges as a useful approach for economic geology.

ACKNOWLEDGEMENTS

The authors wish to thank Dr W. E. L. Minter of the Anglo American Corp., Welkom, South Africa, for collecting the samples and explaining to one of us (B. N.) the petrology and structure of the Vaal Reef in two mines. Professor D. A. Pretorius of the Economic Geology Research Unit at the University of the Witwatersrand, South Africa, provided continued advice and suggestions. Professor C. Steelink, The University of Arizona, assisted in obtaining the electron paramagnetic resonance spectra, and Mr M. H. Engel, The University of Arizona, critically read the manuscript. Financial support was provided by the Chamber of Mines, South Africa, through the Economic Geology Research Unit, University of the Witwatersrand.

REFERENCES

1. NAGY, B., ZUMBERGE, J. E., and NAGY, L. A. Abiotic, graphitic microstructures in a micaceous meta-quartzite ~ 3760 m.y. old from Southwestern Greenland: Implications for early Precambrian microfossils. *Proc. Natl. Acad. Sci. USA*, vol. 72, 1975, pp. 1206-1209.
2. PHILIP, R. P., CALVIN, M., BROWN, S., and YANG, E. Organic geochemical studies on kerogen precursors present in recently deposited algal mats and oozes. *25th International Geological Congress, Sydney, Australia, Abstracts*, vol. 1, 1976, p. 253.
3. NAGY, B. Organic chemistry on the young earth. Evolutionary trends between $\sim 3,800$ million years and $\sim 2,300$ million years ago. *Naturwissenschaften*, vol. 63, 1976, pp. 499-505.
4. ZUMBERGE, J. E., and NAGY, B. Alkyl substituted cyclic ethers in 2,300 myr old Transvaal algal stromatolite. *Nature*, vol. 255, 1975, pp. 695-696.
5. NAGY, L. A., and ZUMBERGE, J. E. Fossil micro-organisms from the approximately 2800 to 2500 million-year-old Bulawayo stromatolite: Application of ultramicrochemical analyses. *Proc. Natl. Acad. Sci. USA*, vol. 73, 1976, pp. 2973-2976.
6. NAGY, B., *et al.* Indications of a biological and biochemical evolutionary trend during the Archean and early Proterozoic. *Precambrian Res.*, vol. 5, 1977, pp. 109-120.
7. PRETORIUS, D. A. Nature of the Witwatersrand gold-uranium deposits. University of the Witwatersrand, Johannesburg, Economic Geology Research Unit, *Inf. Circ. no. 86*, 1974, 50 pp.
8. NAGY, B., MOHAMMED, M. A. J. and MODZELESKI, V. E. An evaluation of pyrolytic techniques with regard to the Apollo 11, 12, and 14 lunar sample analyses. *Space Life Sci.*, vol. 3, 1972, pp. 323-329.
9. BANDURSKI, E. L., and NAGY, B. The polymer-like organic material in the Orgueil meteorite. *Geochim. cosmochim. Acta*, vol. 40, 1976, pp. 1397-1406.
10. ABELSON, P. H., and HARE, P. E. Recent amino acids in the Gunflint chert. *Carnegie Inst. Wash. Yrbk*, 1967-1968, vol. 67, 1969, pp. 208-210.
11. NAGY, B. Porosity and permeability of the Early Precambrian Onverwacht chert: Origin of the hydrocarbon content. *Geochim. cosmochim. Acta*, vol. 34, 1970, pp. 525-527.
12. SMITH, J. W., SCHOPF, J. W., and KAPLAN, I. R. Extractable organic matter in Precambrian cherts. *Geochim. cosmochim. Acta*, vol. 34, 1970, pp. 659-675.
13. SANYAL, S. K., KVENVOLDEN, K. A., and MARSDEN, S. S. Permeabilities of Precambrian Onverwacht cherts and other low permeability rocks. *Nature*, vol. 232, 1971, pp. 325-327.
14. SIMMONDS, P. G., SHULMAN, G. P., and STEM-BRIDGE, C. H. Organic analysis by pyrolysis-gas chromatography-mass spectrometry. Candidate experiment for the biological exploration of Mars. *J. chromat. Sci.*, vol. 7, 1969, pp. 36-41.
15. HARE, P. E., and ABELSON, P. H. Racemization of amino acids in fossil shells. *Carnegie Inst. Wash. Yrbk*, 1966-1967, vol. 66, 1968, pp. 526-528.
16. AKIYAMA, M. L-amino acid stabilization in Na-Montmorillonite and Precambrian chemical fossils. *The Second ISSOL Meeting*, Kyoto, Japan, Abstract no. I-B-3, 1977, p. 6.
17. ZUMBERGE, J. E., BANDURSKI, E. L., and NAGY, B. Analysis of the polymeric structure of kerogen in a Transvaal stromatolite $\sim 2.3 \times 10^9$ years old. *Geol. Soc. Am. Abstr. with Programs*, vol. 7, 1975, p. 1329.
18. SCHOPF, J. M., and LONG, W. E. Coal metamorphism and igneous associations in Antarctica. *Coal Science*, R. F. Gould, ed., Washington D.C., American Chemical Society, 1966. *Advances in Chemistry Series 55*, p. 193.
19. NANDI, S. P., and WALKER, P. L. Diffusion of argon from coals of different rank. *op cit* (18), pp. 379-385.
20. DUTCHER, R. R., CAMPBELL, D. L., and THORNTON, C. P. Coal metamorphism and igneous intrusives in Colorado. *op cit* (18), pp. 708-723.
21. FLAIG, W. Chemistry of humic substances in relation to coalification. *op cit* (18), pp. 58-68.
22. WITHERSPOON, P. A., and WINNIFORD, R. S. The asphaltic composition of petroleum. *Fundamental Aspects of Petroleum Geochemistry*, Nagy B. and Colombo U., eds. Amsterdam, Elsevier, 1967, pp. 261-297.
23. FRENCH, B. M. Graphitization of organic material in a progressively metamorphosed Precambrian iron formation. *Science*, vol. 146, 1964, pp. 917-918.
24. GORDON, G. E. *et al.* Instrumental activation analysis of standard rocks with high-resolution γ -ray detectors. *Geochim. cosmochim. Acta*, vol. 32, 1968, pp. 369-396.
25. SCHMITT, R. A., LINN, T. A., and WAKITA, H. The determination of fourteen common elements in rocks via sequential instrumental activation analysis. *Radiochim. Acta*, vol. 13, 1970, pp. 200-212.
26. HAMILTON, E. I. The determination of uranium in rocks and minerals by the delayed neutron method. *Earth planet. Sci. Lett.*, vol. 1, 1966, pp. 77-81.
27. HARGRAVES, R. B. Silver-gold ratios in some Witwaters-

- rand conglomerates. *Econ. Geol.*, vol. 58, 1963. pp. 952-970.
28. SCHIDLOWSKI, M. The gold fraction of the Witwatersrand conglomerates from the Orange Free State Goldfield (South Africa). *Mineral. Deposita*, vol. 3, 1968. pp. 344-363.
29. VILJOEN, E. A. An electron-microprobe analysis of gold in the Witwatersrand blanket and in ores from the Barberton Mountain Land, Johannesburg, National Institute for Metallurgy, *Rep. no. 1361*, 1971.
30. MINTER, W. E. L. Sedimentology of the Vaal Reef in the Klerksdorp area. Ph.D. Thesis, Johannesburg, University of the Witwatersrand, 1972.
31. MINTER, W. E. L. Detrital gold, uranium, and pyrite concentrations related to sedimentology in the Precambrian Vaal Reef placer, Witwatersrand, South Africa. *Econ. Geol.*, vol. 71, 1976. pp. 157-176.
32. HASKIN, L. A., and FREY, F. A. Dispersed and not-so-rare earths. *Science*, vol. 152, 1966. pp. 299-314.
33. WILDEMAN, T. R., and HASKIN, L. A. Rare earths in Precambrian sediments. *Geochim. cosmochim. Acta*, vol. 37, 1973. pp. 419-438.
34. CORYELL, C. D., CHASE, J. W., and WINCHESTER, J. W. A procedure for geochemical interpretation of terrestrial rare earth abundance patterns. *J. geophys. Res.*, vol. 68, 1963. pp. 559-556.
35. HASKIN, L. A., et al. Relative and absolute terrestrial abundances of the rare earths. *Origin and distribution of the elements*. L. H. Ahrens, ed. Oxford, Pergamon, 1968. pp. 889-912.
36. ROALDSET, E. Rare earth element distributions in some Precambrian rocks and their phyllosilicates, Numedal, Norway. *Geochim. cosmochim. Acta*, vol. 39, 1975. pp. 455-469.
37. RONOV, A. B., BALASHOV, Yu. A., and MIGDISOV, A. A. Geochemistry of rare earth elements in the sedimentary cycle. *Geokhimiya*, no. 1, 1967. pp. 3-19.
38. NAGASAWA, H. Rare earth concentrations in zircons and apatites and their host dacites and granites. *Earth planet. Sci. Lett.*, vol. 9, 1970. pp. 359-364.
39. CULLERS, R. L. et al. Rare earth distributions in clay minerals and in the clay-sized fraction of the Lower Permian Havensville and Eskridge shales of Kansas and Oklahoma. *Geochim. cosmochim. Acta*, vol. 39, 1975. pp. 1691-1703.
40. CULLERS, R. L. et al. Rare earth elements in Silurian pelitic schists from N. W. Maine. *Geochim. cosmochim. Acta*, vol. 38, 1974. pp. 389-400.
41. HALLBAUER, D. K. The plant origin of the Witwatersrand 'carbon'. *Minerals Sci. Engng*, vol. 7, 1975. pp. 111-131
42. NAGY, L. A. Comparative micropaleontology of a Transvaal stromatolite ($\sim 2.3 \times 10^9$ y. old) and a Witwatersrand carbon seam ($\sim 2.6 \times 10^9$ y. old). *Geol. Soc. Am. Abstr. with Programs* vol. 7, 1975. pp. 1209-1210.
43. WILDEMAN, T. R., and CONDÉ, K. C. Rare earths in Archean graywackes from Wyoming and from the Fig Tree Group, South Africa. *Geochim. cosmochim. Acta*, vol. 37, 1973. pp. 439-453.
44. RÖGERS, J. J. W., and ADAMS, J. A. S. Thorium. *Handbook of geochemistry*. Wedepohl, K. H. ed. New York, Springer, 1974, vol. 2, part 4, sect. 90.
45. BREGER, I. A., DEUL, M., and RUBINSTEIN, S. Geochemistry and mineralogy of a uraniferous lignite. *Econ. Geol.*, vol. 50, 1950. pp. 206-226.
46. MOORE, G. W. Extraction of uranium from aqueous solution by coal and some other materials. *Econ. Geol.*, vol. 49, 1954. pp. 652-658.
47. SZALAY, A. Cation exchange properties of humic acids and their importance in the geochemical enrichment of UO_2^{+2} and other cations. *Geochim. cosmochim. Acta*, vol. 28, 1964. pp. 1605-1614.
48. KOLODNY, Y., and KAPLAN, I. R. Deposition of uranium in the sediment and interstitial water of an anoxic fjord. *Symposium on hydrogeochemistry and biogeochemistry, Tokyo, Sept. 1970. Proceedings*. Washington, Clark Co., 1973. vol. 1 - *Hydrogeochemistry*. pp. 418-442.
49. SCHIDLOWSKI, M. Ore-microscopic observations on uranium-bearing constituents of the Witwatersrand conglomerates. *The genesis of uranium- and gold-bearing pre-cambrian quartz-pebble conglomerates*. Golden, Colorado, Geological Society of America, 1975.
50. FEATHER, C. E., and KOEN, G. M. The mineralogy of the Witwatersrand Reefs. *Minerals Sci. Engng*, vol. 7, 1975. pp. 189-224.
51. ONISHI, H. Antimony. *Handbook of geochemistry*. Wedepohl, K. H. ed., New York, Springer, 1974 vol.2, part 4, sec. 51.
52. HALLBAUER, D. K., and VAN WARMELO, K. T. Fossilized plants in thucholite from Precambrian rocks of the Witwatersrand, South Africa. *Precambrian Res.*, vol. 1, 1974. pp. 199-212.
53. WOLK, C. P. Physiology and cytological chemistry of blue-green algae. *Bacteriol. Rev.*, vol. 37, 1973. pp. 32-101.
54. AUSTEN, D. E. G. et al. Electron spin resonance study of pure macerals. *op cit* (18). pp. 344-362.
55. STEELINK, C. Electron paramagnetic resonance studies of humic acid and related model compounds. *op cit* (18). pp. 80-90.
56. NAGY, B. *Carbonaceous meteorites*. Amsterdam, Elsevier, 1975. p. 315.
57. HUANG, R. L., GOH, S. H., and ONG, S. H. *The chemistry of free radicals*. London. Edward Arnold, 1974. 244 pp.
58. BOVEY, F. A. *The effects of ionizing radiation on natural and synthetic high polymers*. New York, Wiley Interscience, 1958. 287 pp.
59. ARENA, V. *Ionizing radiation and life*. St. Louis, C. V. Mosby, 1971. 543 pp.
60. DESROSIER, N. W., and ROSENSTOCK, H. M. *Radiation technology in food agriculture, and biology*. Westport, Conn., AVI, 1960. 401 pp.
61. GETOFF, N. Radiation chemistry of amino acids. *Biological Effects of Transmutation and Decay of Incorporated Radioisotopes, Proceedings of a Panel, Vienna*. 1967 Vienna, International Atomic Energy Agency, 1968. pp. 215-231.
62. ADHIKARI, H. R., and TAPPEL, A. L. Fluorescent products from irradiated amino acids and proteins. *Radiat. Res.*, vol. 61, 1975. pp. 177-183.
63. FARAGGI, M., and TAL, Y. The reaction of the hydrated electron with amino acids, peptides, and proteins in aqueous solution. II Formation of radicals and electron transfer reactions. *Radiat. Res.*, vol. 62, 1975. pp. 347-356.
64. EHRENBERG, A. Research on free radicals in enzyme chemistry and in radiation biology. *Symposium on Free Radicals in Biological Systems, Stanford University, 1960. Proceedings*, Blois, M. S., et al. eds. New York, Academic, 1961. pp. 337-350.
65. PHILLIPS, G. O. Radiation effects on carbohydrates. *Energetics and Mechanisms in Radiation Biology*. Phillips, G. O., ed. New York, Academic, 1968. pp. 131-152.
66. CANNISTRARO, S., LION, Y., and VAN DE VORST, A. Formyl radicals in X-irradiated frozen aqueous solutions of DNA and nucleic acids constituents. *Radiat. Res.*, vol. 64, 1975. pp. 581-592.
67. NAPIER, K. H., and GREEN, J. H. The action of ionizing radiation on simple organic compounds. *Radiation Biology, Proceedings of the 2nd Australasian Conference on Radiation Biology, Melbourne*, 1958. Martin, J. H. ed., London, Butterworths, 1959. pp. 87-94.
68. DILLI, S., and GREEN, J. H. Synthesis of organic compounds by ionizing radiation. *op cit* (67). 1958. Martin J. H. editor. pp. 103-116.
69. LING ONG, H., and SWANSON, V. E. Natural organic acids in the transportation, deposition and concentration of gold. *Colo. Sch. Mines Q.*, vol. 69, 1974. pp. 395-425.